NUMERICAL STUDY ON THE SEISMIC PERFORMANCE OF HYBRID STEEL MOMENT FRAMES WITH CLT BALLOON SHEAR WALLS

by

Mehdi Khajehpour

M.Sc., Sharif University of Technology, 2013

THESIS SUBMITTED IN PARTIAL FULFILLMENT OF
THE REQUIREMENTS FOR THE DEGREE OF
MASTER OF APPLIED SCIENCE
IN
NATURAL RESOURCES AND ENVIRONMENTAL STUDIES

UNIVERSITY OF NORTHERN BRITISH COLUMBIA

August 2020

Abstract

A proposed hybrid lateral load resisting system combining a moderately ductile steel moment resisting frame (SMRF) with Cross-laminated Timber (CLT) balloon-framed shear walls is investigated on 8, 12 and 16-storey case-study buildings using equivalent static, linear dynamic (modal), nonlinear static (push-over) and nonlinear dynamic (time history) analyses. First, a SMRF is designed using ETABS, then the hybrid structures are analysed in OpenSees. By adding the CLT shear wall to steel moment frame, the period of structure decreased and its stiffness increased. The time history analyses result revealed that by adding the CLT shear wall the maximum drift decreased, while the maximum base shear in hybrid structure slightly increased. The hold down uplift forces under earthquake records are reported and compared to each other. Using push-over capacity-curves, a ductility reduction factor of 3.6, an over strength factor of 1.57 and a seismic response modification factor of 5.67 are derived.

Table of Contents

List of Tables

List of Figures

Acknowledgments

I would like to express my sincere gratitude to my supervisor, Dr. Thomas Tannert for his support during the journey of my graduate education: for flawless teaching of courses as well as his guidance and leadership on my thesis. He is an exceptional supervisor and scientist and more importantly a great person. He has not just thought me the knowledge but he also how to be passionate, responsible for my future career.

Besides my Supervisor, I would like to thank the other members of my supervisory committee: Dr. Asif Iqbal, Dr. Cristiano Loss, Dr. Marjan Popovski, and in particular Dr. Yuxin Pan for their insightful comments.

In addition, a thank to my friends, Amir Hasanpour, Hossein Mohammadi, Mohammad Yekrangnia and Yuxin Pan for helping me with their novel ideas and answering my inquiries during the thesis.

My sincere thanks also go to Dr. Roger Wheate and all UNBC faculty and staff helping me out with all my queries during my graduate studies.

Lastly, I would like to thank my parents and wife for their love and support throughout my life.

1 Introduction

1.1 Motivation

Hybrid structures are innovative solutions for structural engineering problems. Engineers employ hybridization to alleviate the weaknesses of one material via exploiting the strength of another (Bhat, 2013). One of the most common hybridizations in structural engineering is reinforced concrete. Over the past decades, engineers have designed multiple tall buildings using this method to provide necessary structural strength against lateral and gravity loads.

A common renewable construction material employed in many parts of the world is wood. Due to its renewable trait, it has increasingly gained attention among developers (NRC, 2018). In addition to conventional light wood frame construction, mass timber is applied increasingly, also in applications related to tall buildings (FII, 2014). Mass timber construction employs large and pre-fabricated engineered wood members in various parts of the construction. Glue-laminated Timber (Glulam), Cross-laminated Timber (CLT), Nail-laminated Timber (NLT), and Dowel-laminated Timber (DLT) are amongst the wood products known in mass timber (FII, 2014).

CLT is a considerable innovation; it is applicable to many parts of mass timber buildings, including floor systems, diaphragms, roof systems, and shear walls (Karacabeyli & Gagnon, 2019). The Wood Innovation Design Center, located in Prince George, British Columbia, Canada, is one example of constructions where CLT is employed as shear wall to provide resistance against lateral loads (CWC, 2015). In CLT walls, two types of construction can be utilized, namely platform-type, and balloon-framing type (Karacabeyli & Gagnon, 2019). Previous research on CLT shear walls had mainly focused on platform-type construction, while few studies have considered CLT balloon-framing.

Steel moment-resisting frames (SMRF) are common lateral load resisting systems (LLRS) utilized in steel structures. In midrise and high-rise buildings, the major difficulty of LLRS is the high lateral displacement that controls the design of the members. One challenge in the design of steel moment frames is satisfying drift criteria under lateral loads. Structural members have the proper strength to carry the forces but cannot satisfy the drift limiting criteria. By adding a bracing system or shear wall, a hybrid lateral load system is formed capable of limiting the drift.

One solution to control the drift in high-rise structures with steel moment frames is utilizing CLT panels as shear walls and constructing a hybrid structure with a hybrid LLRS. Adding the balloon-framed CLT shear walls to a steel structure enables the design and construction of efficient tall buildings. However, since such a hybrid system is not included in the National Building Code of Canada, it would have to be designed using seismic ductility force reduction factor (R_d) of the lower ductility system, herein balloon-framed CLT shearwalls, with R_d = 1.3. Therefore, it is of interest to understand the behaviour of dual LLRS in a hybrid building to improve the design efficiency and performance of the structure.

1.2 Objectives

The main objective in this research is evaluating the seismic performance of a hybrid structure with two LLRS consisting of steel moment frames and CLT shear walls, in terms of storey drift, period, and base shear in comparison to a pure SMRF. The secondary objective is to propose system ductility and over-strength factors to be applied to this hybrid LLRS structure.

1.3 Thesis Overview

In Chapter 2, important material properties of steel and timber (including CLT), along with types of hybridization and different timber and steel LLRS is reviewed. In Chapter 3, methods for

structural analysis, including the equivalent static procedure, modal response spectrum analysis, pushover analysis, and nonlinear dynamic (time history) analysis are reviewed. A case study for a steel moment frame building and its design procedure using NBCC, along with its modal response spectrum are described and analyzed in Chapter 4. Subsequently, CLT shear walls are added to the steel moment frame to form a hybrid structure. Modal analysis is applied to steel moment-resisting and hybrid models to compare periods and mode shapes. To determine the over-strength (Ω) and period-based ductility (μ_T), the hybrid structure is modelled in OpenSees with nonlinear static pushover analysis through the FEMA P695 procedure. Non-linear dynamic analyses are performed on steel moment-resisting and hybrid models using 10 linearly-scaled Vancouver hazard response spectrum ground motions. In Chapter 5, the results of the modal, push-over, and time history analysis, as well as the proposed ductility and over-strength factors for the hybrid building are presented. Finally, in Chapter 6, the thesis is concluded and recommendations for future work are suggested.

1.4 Scope and Limitation

The presented research covers the seismic evaluation of the Hybrid CLT-Steel structure. Fire design, cost estimation, and constructability of this building are out of the scope of this research. The contribution of this thesis is limited to 8, 12, and 16-storey buildings with an asymmetric plan, located in Vancouver, Canada. The connections employed in CLT panels are HSK only. Seismic modification factors for the Hybrid models are determined according to push-over analysis, FEMA P695 and incremental dynamic analysis are not taken into consideration. The seismic performance of the structure is investigated through 2D models only.

2 Literature Review

2.1 Timber, Steel and Hybrid Building Materials

For designing a hybrid structure and to utilize each material in a way that weakness of one material can covered by the other's strength, understanding of each material and its relevant properties is required. Steel is an isotropic material with the same mechanical properties in all directions. Timber, in contrast, is an orthotropic material, which means that its properties are different in the three mutually perpendicular axes. In structural applications, the mechanical properties of timber are defined as parallel to the grain and perpendicular to the grain (Khorasani 2010). Timber is a hygroscopic material that absorbs and loses moisture from the environment. This character of Timber causes a dimensional change which differs for grain orientation and Timber species. However, moisture has no effect on dimensional changes of steel (Slavid 2005; Khorasani 2010). Table 2.1 presents some relevant mechanical properties of steel and timber.

Table 2.1 Material properties for steel and timber (CSA O86, 2016; ASTM, A992, 2015)

Material	Yield Strength (MPa)	Density (kg/m^3)	Elasticity Modulus (MPa)	Compressive Strength (MPa)	Tensile Strength (MPa)
Steel (ASTM A992)	345	7850	200000	450	450
D-Fir-L 24f-E Glulam	N/A	400-600	12800	Parallel 30.2 Perp. 7*	Parallel 7 Perp. 0.83

2.1.1 Cross Laminated Timber

One of the innovations in the field of engineered wood products is CLT. CLT panels are made of several layers of orthogonally glued lumber boards to form a solid panel, see Figure 2.1. These panels can be used as floors, roofs, as well as compartment and shear walls. Using CLT has many

advantages: mass production, prefabrication, speed of construction, acoustic performance and thermal insulation are some of them (Karacabeyli & Gagnon, 2019; Ceccotti, 2008).

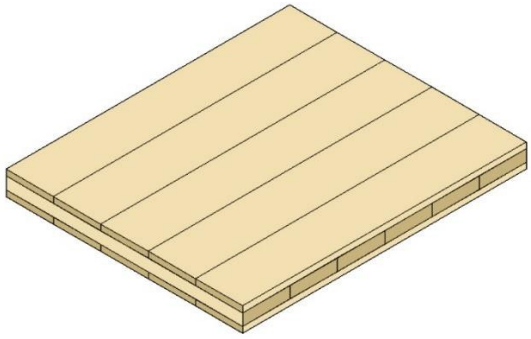

Figure 2.1 CLT Panel

2.1.2 CLT Construction

CLT structures can be built in two ways: platform-type construction and balloon-type framing. In platform construction, each floor is a platform for they storey above with the walls attached to the foundation and the floors by steel brackets and hold-downs (HDs). One of the drawbacks of platform construction are the compression perpendicular to grain stresses which limit the number of storeys. In Balloon framing, the walls are continuous and there is no storeys limitations caused by compression perpendicular to grain strength. To resist against uplift, HDs are required and to resist against sliding, shear brackets or similar connections. Since the focus of previous research on CLT construction has been mostly on platform-type construction, more studies related to balloon-framing are required.

2.1.3 Sustainability and Environmental Impact of Timber Construction

The world population is growing fast and it is expected to increase at a rate of 1.2 % annually. (United Nation, 2015). With this rapid increase, urbanisation, and the increase in carbon footprint the demand for sustainable material in construction is seen in populated areas. A comparison of a

wood house with sheet metal and concrete houses in six key environmental measures: embodied energy, global warning potential, air toxicity, water toxicity, weighted resource use, and solid waste use showed that the wood frame house has lower impacts on the environment for five of the six key measures (CWC, 2004). Comparisons of construction costs between timber, steel, and concrete for four different types of buildings showed that in all four types, timber construction was cheaper ranging from 2 to 14% (Dunn, 2015). Because of the decrease in on-site labour costs, mass timber construction is more economical (Kremer & Symmons 2015). Since in wood construction many components are prefabricated, the on-site construction time is often less than for concrete construction. By considering the increasing rate in urbanization the tall wood building is the most sustainable solution to answer the housing need of the increasing population.

2.1.4 Hybridization of Materials

A hybrid system is a system in which two or more materials are combined to utilize the strength of each component and cover weaknesses. Hybridization can be implemented at three-levels: component level, system-level, and building level. Common examples of component level hybridization are hybrid slabs, beams and columns. For example, in a flitch beam steel plates are locate between timber members. The steel beam has higher strength in comparison to timber plates and the timber beams provide resistance against lateral buckling. An example of system-level hybridization is a steel timber truss, where the top chord is made of timber and the bottom chord is made of steel which has a good performance in tension. Building level hybridization combines different structural systems for example the lower storeys being made of concrete and the upper storeys made of a wood frame structure (Dickof, 2013).

2.2 Lateral Load Resisting Systems

The loads applied to a building can be divided into gravity loads and lateral loads. The lateral load can be caused by an earthquake or wind. The LLRS is the part of a structure designed to withstand the lateral loads and carry them through a safe load-path to the foundation. Multiple LLRS are available to provide lateral stability and rigidity for structures. In taller structures, engineers often face a challenge to satisfy the required demands for drift and strength, while minimizing the effect on architectural components. The main LLRSs frequently used in steel and timber construction can be categorized into the following categories: i) Steel Moment Frames; ii) Steel Braced Frames; iii) Light wood frame shear walls iv) CLT shear walls; and v) Hybrid Steel Timber LLRS.

2.2.1 Steel Moment Resisting Frames

Steel moment resisting frames (SMRS) include a series of beams and columns and rigid connections that carry both the lateral and gravity forces (Figure 2.2). In this system, since there are no additional lateral force-resisting members (such as braces or shear walls), the structure is highly ductile; in other words, by applying lateral forces, the frame of the structure is deformed and thus prevents collapse. Moment frames are often used in low- to mid-rise structures. An advantage of moment-resisting frames is the open bays that allow for flexible design and open space in architecture planning.

But moment frame structures also have several disadvantages. The rigidity of connections requires field welding or costly connections with multiple bolts. Moment frames also require larger members cross-sections compared to other systems which increase the cost of construction. Since the gravity load and lateral load are resisted by the same members, beams and girders need to be changed on each floor which causes more design effort (Chok, 2004). Further, this system is only

practical for low- and mid-rise structures and cannot be used in high rises where the need for large members to satisfy the drift requirements is inevitable. The amount of steel required to satisfy drift criteria for a structure with a height to length ratio of 2 is three times greater than the amount of steel required to satisfy the strength criteria (Chok, 2004).

Figure 2.2 Moment Frame (https://sabzsaze.com/moment-frame/)

2.2.2 Steel Braced Frames

In a braced frame system, beams are connected to a column with hinge connections and the flexural stiffness of the beams is not involved in the absorption of lateral forces. This system carries the gravity loads by means of beams and columns; to provide lateral resistance and stability, diagonal members and bracing are used. Braced framing can be designed into a single storey height or multi-storey height belt trusses for buildings from low-rise to high-rise.

Using the braced frame system has many advantages. The bracing system converts lateral loads to axial load in diagonal members which is more efficient than bending in a moment resisting frame. Designing and casting frame while the lateral system is separated from the gravity system is much easier and more convenient to do. Also because of simple hinge connections, heavy field welding and bolting is not required which leads to cheaper construction (Chok, 2004). The biggest problem of a braced frame is its incompatibility with many architectural designs. Bracing in bays conflict with open space in plans, see **Error! Reference source not found.**. Although diagonal members

fill the bays, separating the lateral resisting system and gravity system leads to more column spacing in interior design thus it increases the flexibility of interior designing into the storey level.

Figure 2.3 Casino Barcelona. Barcelona, Spain (photo by Miguel Machado on unsplash.com)

Chok also studied the effect of building height on the volume of steel needed for braced frame and moment frame systems on a 30-storey building. Table 2.2 shows the difference in the volume of steel in a 30-storey structure for satisfying the same deflection criteria. This table is normalized with the result of the 10-storey structure (Chok, 2004). In a 30-storey structure, the braced frame uses almost 5 times less steel than the moment-resisting frame. This fact explains why most of the tall building uses a bracing system for lateral resisting system. As an example, The John Hancock building in Chicago uses 145 kg/m^2steel per unit area; however, the height of the building is 8 times bigger than its plan dimensions (Chok, 2004).

Table 2.2: Comparison of Steel Volume Required (Chock, 2004)

				Moment Frames		Braced Frames	
Storeys	Height	Aspect Ratio	Deflection Criteria (m)	Strength Based Steel Volume (m^3)	Stiffness Based Steel Volume (m^3)	Single Bay Bracing	3 Bay Wide Bracing
30	105	3	0.21	65.3	219	88.79	47.87
Normalized Steel Volume				7.47	25.06	10.16	5.48

2.2.3 Light-frame Wood Construction

The most common structural system used in North America is light-frame wood frame construction where the LLRS consist of wood shear walls. In this system, lateral loads are transferred to the foundation by shear walls consisting of stud walls with nailed Plywood and oriented strand board (OSB) sheathing. The sheathing behaves elastically under the lateral loads but the nailed connections are designed to deform plastically. Lightwood frame walls have a good performance in seismic design. Because of their lightweight, they attract lower earthquake energy and seismic forces. Their numerous nailed connections provide ductility and the repetitive members and connections increase the structural redundancy and provide a proper load path for transferring the lateral forces (rethink wood, 2015). In light wood frame shear walls to avoid uplift and rocking in walls and increasing the overturning resistance and ductility, HDs are installed at the corners of walls (Yasumura, 2000). Studies on the failure mode of light wood frame shear walls revealed that the failure mode of these walls changes from one-storey to six-storey. For one storey the major failure occurs in connections or shear failure but for six-storey belongs to studs and it is flexure failure (Mostafaei et al, 2013).

2.2.4 CLT Shear Wall

With the increased use of CLT, many studies have focused on CLT as a LLRS. CLT panels in shear walls have rigid body behaviour during in-plane loading and all deformation occurs in connections between panels themselves and panels and main structure. Thus, the resistance of CLT shear walls is governed by its connectors. While dissipative connections should have enough ductility, the non-dissipative connections should remain elastic. The panels' resistance should be higher than the ultimate resistance of dissipative connection (Karacabeyli & Gagnon, 2019).

The primary research on CLT as a LLRS systems performed in Europe. The SOFIE project is the most comprehensive study on the static, acoustic, and seismic behaviour of CLT. It comprised test on different kinds of connections, quasi-static experiments on CLT walls, pseudo-dynamic tests on one storey CLT structure and a full-scale shaking table test on three and seven-storey structure (Ceccotti et al, 2006a, 2006b, 2008, 2010 and 2013). Popovski et al. (2010) performed a series of 32 monotonic and cyclic experiments with a different arrangement of openings in walls and different sizes of CLT panels. The experiments confirmed the CLT panels' rigid behaviour and demonstrated that the majority of the deformation happens in the steel brackets and inter-panel connectors. Pei et al. (2013) evaluated the seismic modification factor for CLT buildings. They designed a 6-storey CLT shear wall structure using a simplified kinematic model with a performance-based design procedure the response modification factor 4.5 proposed for the system while designing according to ASCE 7-10.

There is no research on estimating seismic modification factors of CLT balloon framing LLRS system that can be used in NBCC (Karacabeyli & Gagnon, 2019). The seismic modification factors in Canadian codes just include platform construction that are stated in CSA O86. In this provision, The $R_d \leq 2$ and $R_o=1.5$ are quantified for platform construction where energy dissipate through connections (CSA O86, 2016).

2.2.5 Wood Hybrid Lateral Load Resisting Systems

Hybrid systems can be used to resist lateral and gravity loads and to improve the seismic performance of timber structures. The major advantage in the hybridization of wood with other materials from a seismic design point of view is the lightweight of wood in comparison to other materials which attracts lower seismic forces.

2.2.5.1 Wood-Concrete LLRS

A solution to build tall wood structures and deal with seismic forces is to incorporate concrete in the LLRS to control lateral displacement effectively. Also, if in a wood structure, concrete used as a part of the floor system it could have a good consistency with concrete LLRS and the diaphragm and LLRS work better together for conveying the lateral loads to the foundation. Using concrete cores around the elevators or stairs shaft as an LLRS could build a non-combustible shield in this part of the building for fire emergencies (Karacabeyli & Gagnon, 2019).

The UBC Brock Common, shown in Figure 2.4, is an 18-storey hybrid structure with a typical storey height of 2.8 m and 58.5 m total height to the top of the elevator core parapet. The first storey is a concrete podium to provide large spans in public spaces and the 17 storeys on top of that is a mass timber structure. Two concrete cores with 450 mm thick shear walls carry the lateral loads and gravity loads are carried by Parallam and Glulam columns. Floors are 5-ply CLT with 40 mm concrete topping which acts as a diaphragm. The mass timber superstructure was 7,648 ton lighter than an equivalent concrete structure (Poirier et al, 2016).

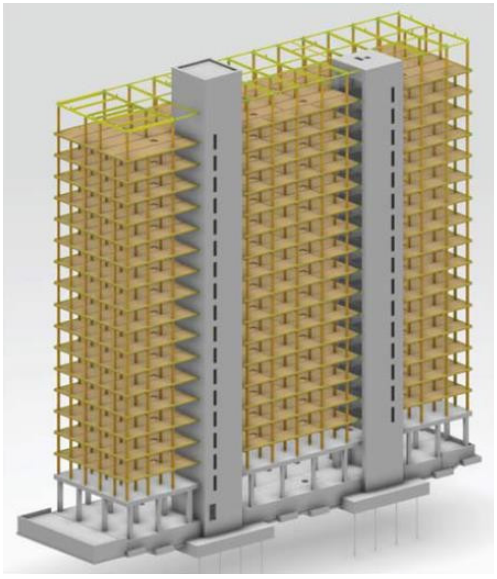

Figure 2.4 Brock Common Building, Courtesy of Fast+Epp (Poirier et al, 2016).

The SOM (2013) Timber Tower research project is a concept for wood-concrete hybrid structures that utilizes mass timber as the main structural material for floors, columns, and shear walls. The building Volume is 70% timber and 30% concrete accounting for the concrete substructure and foundation. The prototypical building is based on an existing concrete benchmark for comparison, the 42-storey Dewitt-Chestnut Apartments building in Chicago. The Glulam column with CLT shear walls and reinforced concrete beams "Concrete Jointed Timber Frame" act as an LLRS system, as shown in Figure 2.5. The CLT shear walls are coupled by reinforced concrete beams to make the whole structure act as a vertically cantilevered beam (SOM, 2013).

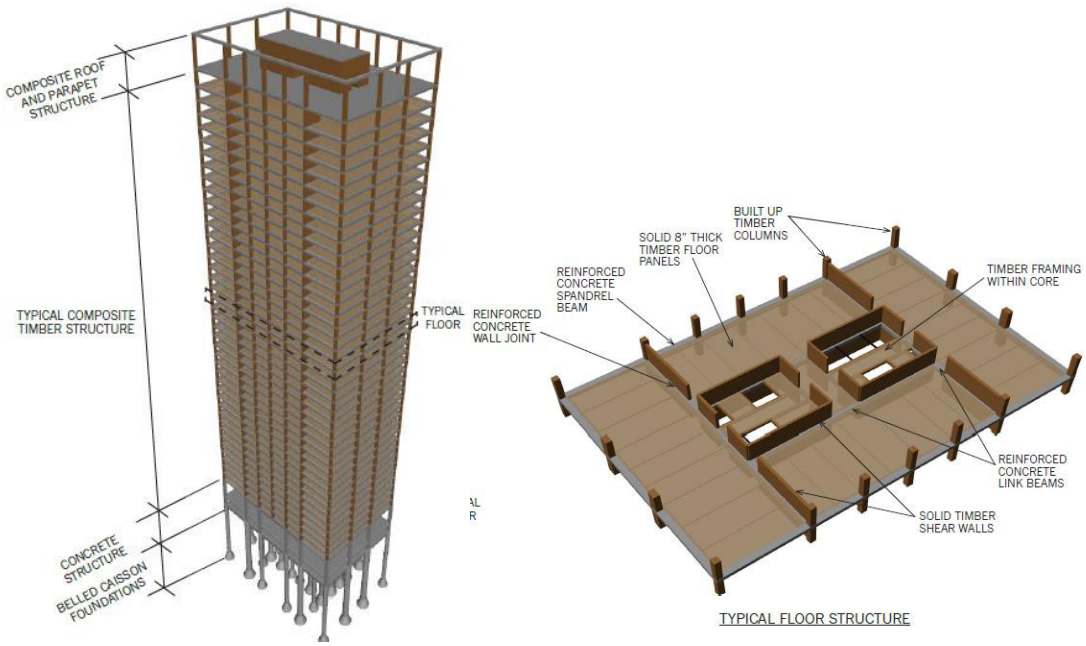

Figure 2.5 SOM Timber Tower Project (SOM, 2013)

2.2.5.2 Wood-Steel LLRS

In wood-steel LLRS as both steel and wood, members are mostly prefabricated so it has less in site labour and reduces the time of construction. One example of hybrid wood steel LLRS systems is the Kanazawa building in Japan (Koshihara et al., 2005). The first storey is reinforced concrete while the second to the fifth storey is a hybrid braced frame using steel and timber (Figure 2.6).

Performance-based design and some test were performed on seismic behaviour of shear walls and buckling of timber steel hybrid systems (Koshihara et al., 2005). All the members made of Glulam with built-in steel to satisfy the structural and fire resistance. The beams are flitch beams and columns are made of wood with steel rods through their centre. The floors are concrete slabs connected to wooden parts using steel plates and screws. Plywood shear walls were screwed to the wood part of columns and beams. On the top and bottom of the wall, the plywood connected to the concrete. In columns, the wood part included two functions that provide fireproofing and restraining the buckling of the steel part. Experiments showed that failure in hybrid columns in which wood part contains steel part under axial loading is in force compression not buckling. Also, the braced member is under lateral load was restrained from buckling by the wood (*Koshihara et al., 2005*).

Figure 2.6 Kanazawa M Building (Koshihara et. al 2005)

Finding the Forest through the Trees (FFTT) (Figure 2.7) is a hybrid steel-timber concept based on balloon framing construction proposed by Green and Karsh for tall building (Green and Karsh, 2012). This system is based on the "Strong Column-Weak Beam" structural concept to withstand the lateral and gravity forces. It consists of Glulam columns and beams, CLT shear walls and steel

beams to provide the ductility through forming plastic hinges. Building with 12, 20 and 30-storeys with different LLRS layouts were analysed in t (Green and Karsh, 2012).

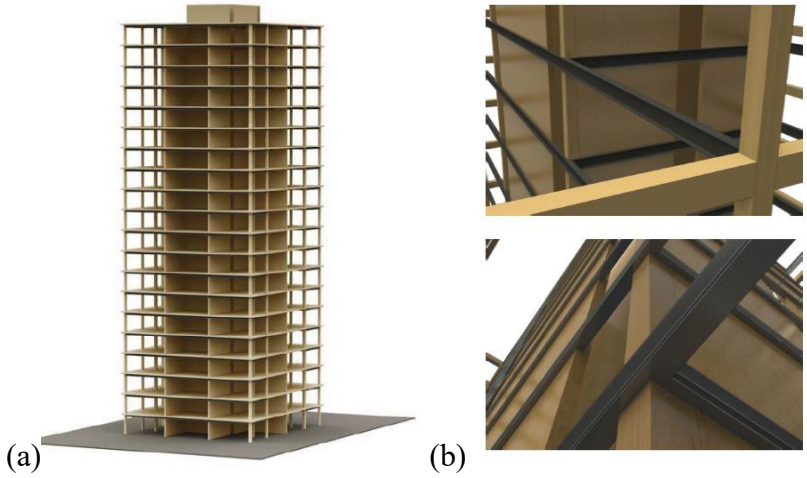

Figure 2.7 a) 20 storey FFTT building; b) FFTT details (Green and Karsh, 2012).

Dickof (2014) studied a CLT-steel hybrid structure at three different height (3, 6 and 9-storey). The CLT panels located in frame bays panels are attached to the frame using steel brackets which provide ductility to the CLT walls. This hybrid system combines high strength and ductility of steel with high stiffness of CLT panels. A 2D nonlinear model was developed in Opensees and the effect of CLT infill wall in both ductile and limited ductile steel moment frame was evaluated. Parametric studies were conducted to evaluate the panel arrangement effect in different bays, Panel thickness and crushing. Push over analysis was applied to estimate over strength and ductility factors based on panel crushing in the link elements and steel yield. Results were revealed infill CLT walls were more efficient in lower ductility steel frames. Ductility factor of 2.5 and an over-strength factor of 1.25 were proposed for the hybrid system according to NBCC.

Tesfamariam et al. (2015) published a design guideline for steel moment resisting frames with CLT infill walls. Three, six and none storey models were designed using force modification factors of R_d=4 and R_o= 1.5. Push-over analyses were performed to validate the overstrength factor; and the

FEMA P695 procedure was applied to evaluate the ductility facto. Incremental Dynamic Analysis (IDA) using Nonlinear Time History Analysis was performed under consideration of 60 ground motion records. Records selected and scaled for city of Vancouver and on the site class C soil according to NBCC 2010. The results showed that R_d=4 and R_o= 1.5 were acceptable for the proposed structural system. Subsequently, Bezabeh et al. (2015a) studied an iterative displacement based design method for the same hybrid steel moment resting frame with CLT infill walls. Nonlinear time history analysis were conducted using 20 earthquake. And finally, Bezabeh et al. (2015b) proposed an equivalent viscous damping-ductility (EVD) law for CLT-infilled steel moment resisting frames. Semi-static cyclic analyses were performed on 243 single storey, single bay hybrid models. Different parameters like the gap between CLT and steel frame, connection spacing, CLT specification and steel post yield behaviour were varied.

2.2.6 Summary of Literature Review

Wood as construction material has the lowest environmental impact compared to other conventional materials like steel and concrete. The many advantages of using wood create a need to build taller wood structures. Lateral forces due to earthquake or wind are resisted by the structures' LLRS. Steel moment frames are commonly used as LLRS. The main drawback to building tall structures with a SMRF is the high lateral displacement of this system under lateral loads. Hybridization is an effective way to use the strength of one material or system to build a taller and more efficient structure. By adding CLT shear walls to SMRF, a wood steel hybrid system with two LLRS is formed. It is postulated that this Hybrid structure can decrease drift and increased stiffness of steel moment resisting structure.

The research gap in the steel wood system with two LLRS points to a demand to research hybrid structural systems which can efficiently use each material specification. The literature review also

shows that mostly the focus of all research on the two types of CLT shear wall construction is on platform construction. However, balloon framing CLT in hybrid structure has many advantages as the installation of CLT is much easier and more practical for construction practice. Therefore, this research aims to focus on the steel CLT hybrid structure in balloon framing construction.

3 Analysis methods of Lateral Load Resisting Systems

3.1 Overview

Structural analysis methods enable calculation of deformation, internal forces, and support reactions for a structure. These methods can be divided into static and dynamic, or linear and nonlinear from another perspective. In linear analysis, the most significant principle is retaining the shape of the member before and after the loading, while maintaining small deformations in the members. In other words, in every step where the member is affected by the load and deformation, the stiffness of the member should not change. This assumption assists in solving the problems and simplifying the formulas, which denotes the inclination of engineers towards using such analysis. In nonlinear analysis, stiffness consistency in the members is no longer assumed, and the stiffness matrix needs to remain dynamic during all stages of loading. As a result of variation in the members' stiffness, the stiffness matrix for the structure will not be constant. By varying the stress and strain in the plastic region, the elasticity modulus of the member changes. Even though this change increases the structural analysis time, it provides more precise results and outputs.

The methods employed in this research are thoroughly discussed in the following sections:

i. Equivalent static-force procedure
ii. Modal response spectrum procedure
iii. Nonlinear static procedure (pushover analysis)
iv. Nonlinear time history analysis

3.2 Equivalent Static Force Procedure

In the equivalent static force procedure (ESFP), the behaviour of the materials is assumed linear, while the earthquake-induced loads are constant (static). The earthquake acceleration force is distributed along the height of the structure (NBCC, 2015). The total lateral force of the earthquake is determined as a coefficient of the building's mass. If the lateral force obtained in this manner is applied to the structure, and the behaviour of the structure is assumed linear elastic, then the resulting deformities will be similar to what is expected in the earthquake. However, if the behaviour of the structure is nonlinear, then the determined forces will be larger than the elastic limit of the material. Therefore, the results of the linear analysis are modified while examining the acceptance criteria in a way to demonstrate nonlinear behaviour during earthquakes. According to the NBCC (2015), the minimum lateral earthquake force, V, is calculated as:

$$V = S(T_a)\, M_V\, I_E\, W / (R_d R_o) \qquad \text{Eq. 3.1}$$

However, V shall not be less than obtained from equation 3.2 for walls, coupled walls, and wall-frame systems and equation 3.3 for moment-resisting frames, braced frames, and other systems:

$$S(4.0)\, M_V\, I_E\, W / (R_d R_o) \qquad \text{Eq. 3.2}$$

$$S(2.0)\, M_V\, I_E\, W / (R_d R_o) \qquad \text{Eq. 3.3}$$

For buildings located on sites other than class F with SFRS with R_d equal to, or greater than, 1.5, the value for V should not be more than the maximum value from either equation 3.4 or 3.5:

$$\frac{2}{3} S(2.0)\, I_E\, W / (R_d R_o) \qquad \text{Eq. 3.4}$$

$$S(0.5)\, I_E\, W / (R_d R_o) \qquad \text{Eq. 3.5}$$

According to NBCC (2015), the main period for a structure is dependent on its lateral load resisting system and height. For steel moment-resisting frames, the lateral period, T_a is determined as:

$$0.085\ (h_n)^{3/4} \qquad \text{Eq. 3.6}$$

where (h_n) is the height of structure in meters. For shear wall and other structures, it is:

$$0.05(h_n)^{\frac{3}{4}} \qquad \text{Eq. 3.7}$$

As denoted by the NBCC (2015), the range of the applications of the ESFP includes: a) cases where $I_E\ F_a S_a(0.2)$ is less than 0.35, where I_E is the importance factor, F_a is the site coefficient, and $S_a(0.2)$ is spectral response acceleration value at 0.2 sec; b) Regular structures with less than 60 m height and a fundamental period less than 2 sec; c) structures with the structural irregularity of less than 20 m in height with periods less than 0.5 sec in each direction.

Since ESFP does not consider the effects of all vibration modes in the structure (i.e. only the first vibrational mode is considered), its application has restrictions in the height. However, the effect of higher modes in regular-shaped low-rise structures is not significant. Generally, static analysis methods are appropriate in cases where the structure response during an earthquake is mainly due to vibrations in the first mode. Hence, on high-rise and irregular buildings, it is necessary to use dynamic analysis methods.

3.3 Modal Response Spectrum Procedure

In modal response spectrum procedure (MRSP), dynamic analysis is performed with the assumption of linear behaviour from the structure via employing the maximum response from all vibration modes of the structure with a significant effect on the total response. The number of vibrational modes in the spectrum analysis should be chosen so that the total percentage for the

effective mass participation in each direction of the earthquake excitation in the selected mode is at least 90% (ASCE7, 2010). In MRSP, forces and deformations caused by the earthquake are determined using dynamic equilibrium equations for the elasticity model of the structure. In this method, compared with the linear static analysis method, since the dynamic characteristics of the structure are introduced in the analysis, the results are more accurate. However, nonlinear material behaviour is not considered in the model.

In this method, the maximum response for each mode is determined using either the mode period from the standard design spectrum or a site-specific design spectrum. Then, the overall response of the structure is estimated using the statistical composition of the maximum responses for each mode. The equivalent static analysis method is a particular response spectrum method that examines only the first mode of the structure and ignores other modes. This spectrum analysis method is a static method that considers the effects of higher modes in the final construct's response. Hence, it is also called pseudo-dynamical.

According to clause 12.9.1.1 of ASCE 7 (2010), modal analysis is necessary to define the natural vibration modes of the structure. It is allowed for the analysis to contain a minimum number of modes to obtain the combined modal mass participation of at least 90% of the actual mass in each orthogonal horizontal direction of the response. Moreover, according to the clause 12.9.1.3 of ASCE 7 (2010), the response parameters for various modes should be combined using the square root of the sum of the squares (SRSS) method, the complete quadratic combination (CQC) method, the complete quadratic combination method, or using an approved equivalent approach.

3.4 Nonlinear Static (Push-Over) Analysis

Nonlinear static analysis is based on the nonlinear behaviour of the structure's components under monotonic displacement-based lateral load patterns. The purpose of this method is to estimate the nonlinear capacity of the structures in earthquakes. This method is a step-by-step analysis. The structure in this method is pushed gradually under the monitoring of the lateral load, with a specified load pattern and displacement of the control point (i.e. the center of mass at the roof storey). In each step, the internal force of the elements is evaluated. If an element exceeds its elastic range, its stiffness will reduce to form a plastic hinge. The steps are then continued until the plastic hinges spread and the control point is displaced until it reaches a specific value determined by the target displacement codes.

One of the most important results expected from this analysis is determining the load-displacement curve or the capacity curve. These curves are obtained by specifying the base shear and the lateral displacement of the control point in each step. The capacity curve provides insight into the ductile capacity and the failure mechanism of the structure. The strength-reduction factor and over-strength factor for the structure can be obtained from the capacity curve via employing the available guideline. The FEMA P695 (2009) method is a method to investigate the capacity curve. In this research, the seismic coefficient factors (i.e. over-strength and ductility factor) are developed according to this method. According to chapter 6.3 from FEMA P695 (2009), "Figure 3.1 shows an idealized pushover curve and definitions of the maximum base shear capacity, V_{max} and the ultimate displacement, δ_u. V_{max} is taken as the maximum base shear strength at any point on the pushover curve, and δ_u is taken as the roof displacement at the point of 20% strength loss ($0.8V_{max}$).

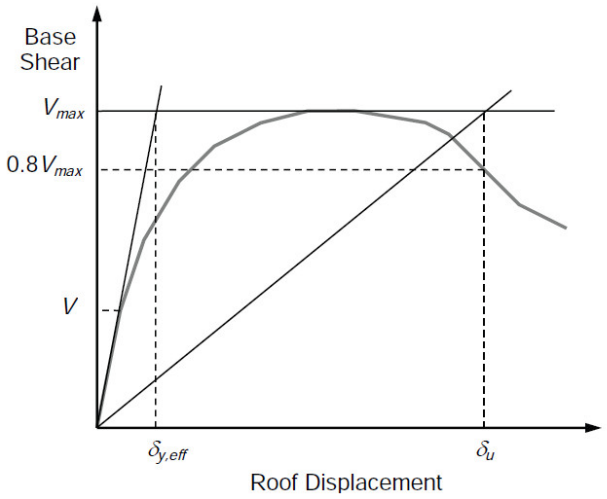

Figure 3.1 Idealized nonlinear static pushover curve (FEMA, 2009)

A nonlinear static pushover analysis is used to quantify V_{max} and δ_u which are then used to compute archetype over strength, Ω and period-based ductility, μ_T In order to quantify these values, the lateral loads are applied monotonically until a loss of 20% of the base shear capacity ($0.8Vmax$) is achieved. The over strength factor for a given index archetype model Ω is defined in equation 3.8 as the ratio of the maximum base shear resistance, V_{max} to the design base shear, V:

$$\Omega = \frac{V_{max}}{V} \qquad \text{Eq. 3.8}$$

The period-based ductility for a given index archetype model, μ_T is defined in equation 3.9 as the ratio of ultimate roof drift displacement, δ_u (defined as shown in Figure 3.1) to the effective yield roof drift displacement$\delta_{y,eff}$:

$$\mu_T = \frac{\delta_u}{\delta_{y,eff}} \qquad \text{Eq. 3.9}$$

The effective yield roof drift displacement is as given by the equation 3.10:

$$\delta_{y,eff} = C_0 \frac{V_{max}}{W}\left[\frac{g}{4\pi^2}\right](\max(T, T_1))^2 \qquad \text{Eq. 3.10}$$

Where C_0 relates fundamental-mode displacement to roof displacement, $\frac{V_{max}}{W}$ is the maximum base shear normalized by building weight, g is the gravity constant, T is the fundamental period, and T_1 is the fundamental period of the archetype model computed using eigenvalue analysis. The coefficient $C0$ is based on Equation C3-4 of ASCE/SEI 41-06, as equation 3.11:

$$C_0 = \varphi_{1,r} \frac{\sum_1^N m_x \varphi_{1,x}}{\sum_1^N m_x \varphi_{1,x}^2} \qquad \text{Eq. 3.11}$$

Where mx is the mass at level x; and $\varphi_{1,x}$ ($\varphi_{1,r}$) is the ordinate of the fundamental mode at level x (roof), and N is the number of levels (FEMA, 2009). The result value for over strength and roof drift calculate from average result of this two driven in the two loading axes.

Defining the relation between $R\mu$ and μ has been the main topic of many researcher in recent years. The complied results of some of them has been stated in conducted researches (Miranda et al, 1994). In this research, two equations have been used for expressing the $R\mu$ and μ relation: a) Newmark and Hall (1982); and b) Lai and Biggs (1980).

Newmark and Hall expressed the ductility reduction factor dependent to period of structure with:

$$R\mu = 1 \qquad (T < 0.3\ s) \qquad \text{Eq. 3.12}$$

$$R\mu = \sqrt{2\mu - 1} \qquad (0.12\ s < T < 0.5\ s) \qquad \text{Eq. 3.13}$$

$$R\mu = \mu \qquad (T > 1s) \qquad \text{Eq. 3.14}$$

Lia and Biggs present the reduction ductility factor dependent of two coefficient of α and β and Period of the structure according to equation 3.15:

$$R\mu = \alpha + \beta (\log T) \qquad \text{Eq. 3.15}$$

α and β are extracted from Table 3.1 based on the structural period and ductility factor (μ).

Table 3.1 factors using in Lia equation (Lia et al, 1980)

		μ			
		2	3	4	5
$0.1s \leq T < 0.5\ s$	α	1.6791	2.2296	2.6587	3.1107
	β	0.3291	0.7296	1.0587	1.4307
$0.5\ s \leq T < 0.7\ s$	α	2.0332	2.7722	3.3700	3.8336
	β	1.5055	2.5320	3.4217	3.8323
$0.7\ s \leq T < 4\ s$	α	1.8409	2.4823	2.9853	3.4180
	β	0.2642	0.6605	0.9380	1.1493

3.5 Non-linear Time History Analysis

In non-linear time history analysis (NLTHA), the structure is loaded with an earthquake acceleration time history (Figure 3.2), while the responses are defined in the form of a time history. The effects of higher modes and variations in the inertial load pattern are considered in relation to the softening of the structure. The maximum total displacement created by an earthquake is determined. However, it is not necessary to estimate this parameter according to the experimental-theoretical relationship. It should be noted that this analysis is very sensitive to variation in the acceleration record characteristics and the nonlinear hardening behaviour of the elements.

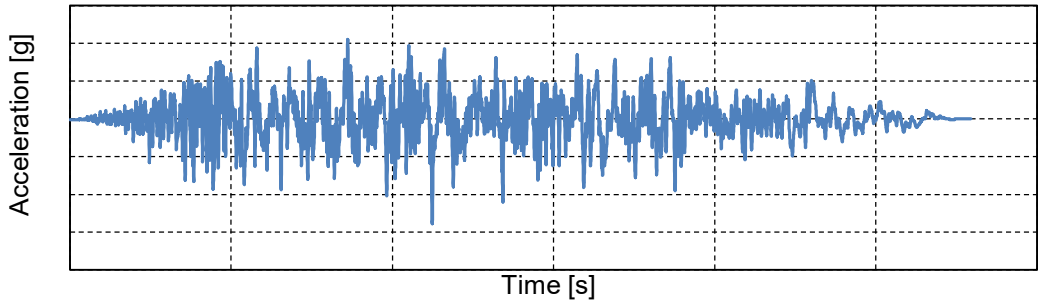

Figure 3.2 Sample acceleration record

Consequently, selection and scaling the earthquake records direct impacts the results. Therefore, to reduce the dispersion of the results and to estimate the seismic requirements accurately, it is

necessary to analyze multiple NLTHA. According to ASCE-7 (2010), the maximum response for 3-6 records or the average response of 7 records or more should be used. Performing NLTHA is compulsory for irregular structures, high-rise buildings, and high-profile structures. Moreover, this analysis can be used for incremental dynamic analysis (Vamvatsikos & Cornell, 2002) and fragility curve development (Moehle & Deierlein, 2004).

In accordance with the ASCE-7 (2010), records employed to determine the effect of ground motion should indicate, as much as possible, the actual movement of the ground at the construction site during the earthquake. Different methods are proposed to scale up the earthquake record, including:

1) Using a proper seismic index (Vamvatsikos & Cornell, 2002): In this method, all earthquake records are directly scaled to a specific equal index. For this purpose, various parameters have been presented in recent years. In specific, parameters such as peak ground acceleration (PGA) and peak ground velocity (PGV) are the most significant parameters considered.

2) *Spectrum scaling (ASCE 7, 2010)*: This method is commonly used for the dynamic analysis of earthquake accelerations records. In this method, the spectrum obtained from the earthquake records is not less than the equivalent design spectrum in a specified period. The range of this period, according to ASCE 7 (2010), is between 0.2T to 1.5 T.

3) Producing the acceleration record in accordance with the target spectrum (NISTGSR, 2011; ASCE 7, 2010): Another method to scale the earthquake records is producing records that fit in the target spectrum, which is generally the ideal spectrum used in the design stage.

4) *FEMA 440 Scaling Method (FEMA, 2005)*: According to this method, the maximum displacement in the center of mass of the roof, obtained using the NLTHA under scaled record, is equal with the target displacement determined from the Pushover analysis.

3.6 Summary on LLRS Analysis Methods

Different methods can be used to analyze and design LLRS. Methods of defining material behaviour and applied loads divide the analysis into linear, nonlinear and static, and dynamic categories. Engineers may employ the appropriate analysis method for specific purposes and/or projects. In the ESFP, material behaviour is linear and does not require dynamic modelling. Therefore, it is a fast-pace analysis. On the other hand, the MRSP method provides good precession since it takes higher modes of vibration into consideration. Consequently, it yields a more efficient and economical design in comparison with the equivalent static procedure.

In nonlinear static (pushover) analysis, the nonlinear behaviour of each member along with the components of the structure are included in the analysis, while instead of applying the specified load, the effect of the earthquake is estimated in terms of deformation. NLTHA is the most accurate method to calculate and investigate the behaviour of the designed structure for a particular earthquake or earthquakes in general. Since earthquakes do not demonstrate similar characteristics, the structure needs to be analyzed under a series of earthquake records, which indicates that the process is time-consuming.

In this research, all the aforementioned analysis methods are applied. The MRSP is used to design the primary cross-sections of the steel moment-resisting frame, while the base shear is estimated using the ESFP method. To estimate seismic modification factors for the proposed hybrid structure, Pushover analysis is conducted according to FEMA P695. NLTHA is performed on the hybrid system to evaluate the effectiveness of adding CLT shear walls to the steel moment-resisting frame.

4 Analysis of Case Study Building

4.1 Overview

This study investigates the effect of adding CLT balloon framing shear walls to a moderately-ductile steel moment-resisting frame (SMRF). In the first step, three SMRF models for 8-, 12- and 16-storey buildings were designed using ETABS (Computer and Structure Inc., 2013). Next, the middle-bay beams were removed and replaced by CLT balloon-framing shear walls to form a structure with Hybrid LLRS (Hybrid). For CLT connections and HDs, HSK were utilized to conduct the analyses as summarized in the flowchart of **Error! Reference source not found.**.

Two-dimensional (2D) models of the Hybrid and SMRF were constructed in OpenSees (MaKenna et al, 2000). To evaluate the period of the structure and initial behaviour, modal analysis was conducted on both sets of models. A push-over analysis was further performed on the Hybrid model to evaluate the seismic modification factors of the hybrid structure. Since the SMRF is already in NBCC, such analyses for this system were not necessary. In order to compare the seismic responses of the Hybrid and SMRF models, NLTHA were conducted using records from 10 earthquakes. Finally, to compare the volume of steel usage in hybrid and SMRF structures, the Hybrid structure was redesigned using ETABS with the new seismic modification factor which proposed from Pushover analysis.

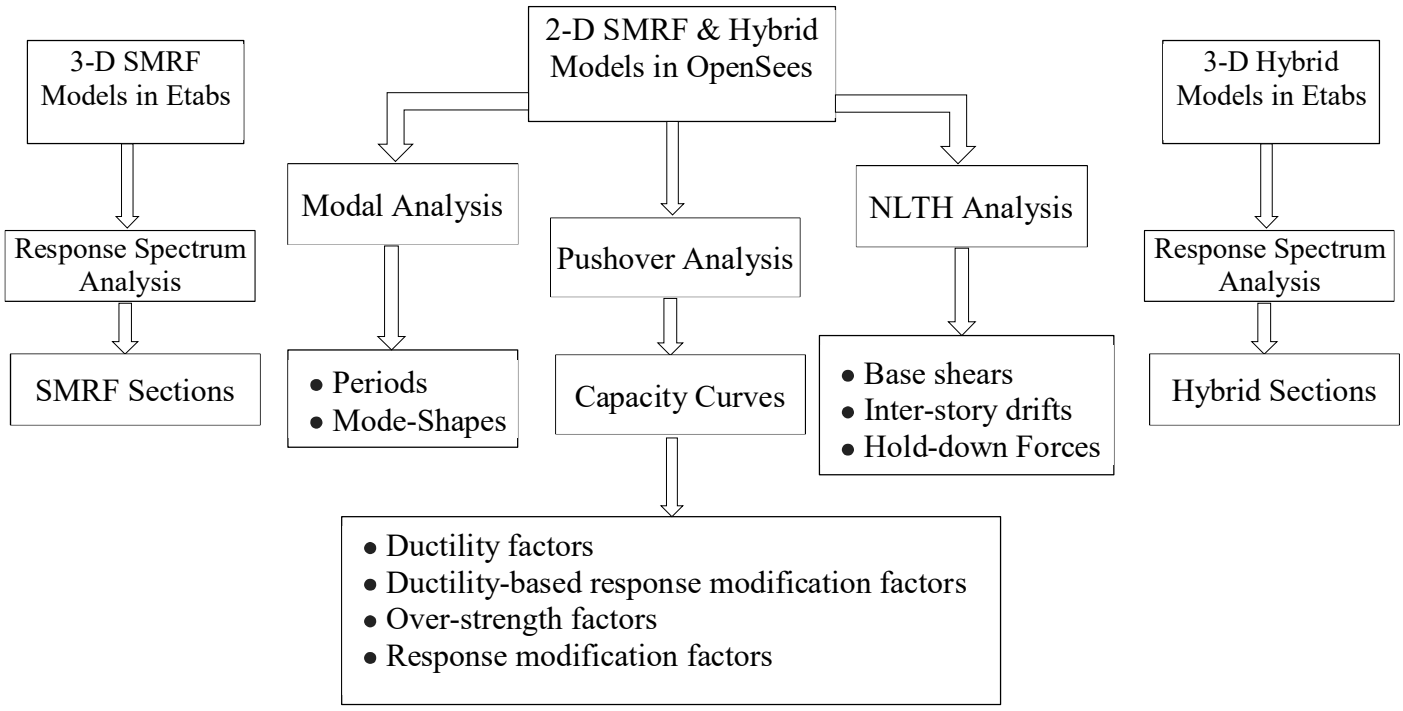

Figure 4.1 Analysis methods flowchart

4.2 Building Description

The considered case study building has an asymmetric plan with three bays, each with 9 m in every direction and 3 meters storey heights (Figure 4.2). The plan dimensions were 27 m by 27 m. Three different building heights, namely 8-storey (24 m), 12-storey (36 m), and 16-storey (48 m) were considered. All floors were made of 175 mm (5-ply) CLT panels with 100 mm concrete topping. In specific, the buildings were residential buildings, located in Vancouver, Canada. The soil type of the site was class C. For the hybrid buildings, CLT shear walls were located in the middle span to form a square core. These CLT panels were 7-ply (245 mm thick), 3 m wide, and 12 m tall, and 3 CLT panels were placed next to each other to fill the 9 m middle span.

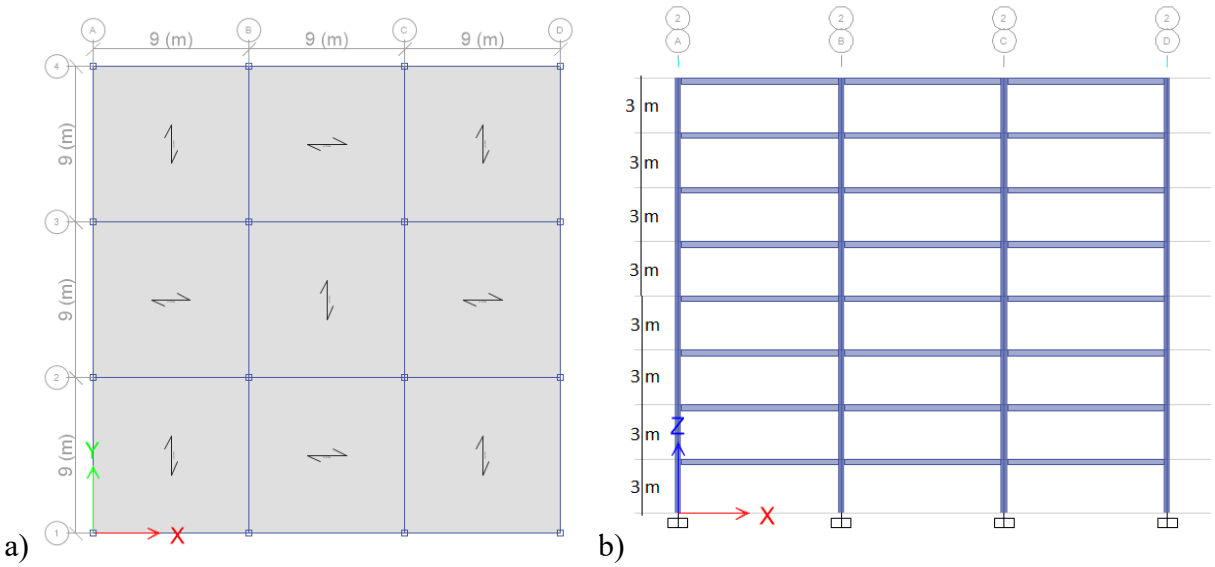

Figure 4.2 a) Building plan b) 8-storey building elevation

4.3 Model Development

To develop the model, first, the 3D models for three SMRF steel structures with 8, 12, and 16 storeys were developed in ETABS. In this step, the design was conducted in accordance with NBCC (2015) and CSA-S16 (2014) provisions to obtain the necessary beam and column sections. Both strength and drift provisions were applied here. The analysis and the design method regarding this step are discussed thoroughly in section 4.5. Moreover, results are shown there and in Appendix A. The plan view and the 3D view for the 8-storey SMRF and Hybrid models are demonstrated in Figure 4.3 and Figure 4.4 respectively.

Next, CLT panels were added to the middle span of the 2D frames and the beams were removed from the middle span. The 2D frame for the SMRF and the Hybrid buildings are shown in Figure 4.5. They were modelled and analyzed in OpenSees, performing modal, pushover, and time history analysis. The overview of all the 6 models is presented in Table 4.1**Error! Reference source not found.**.

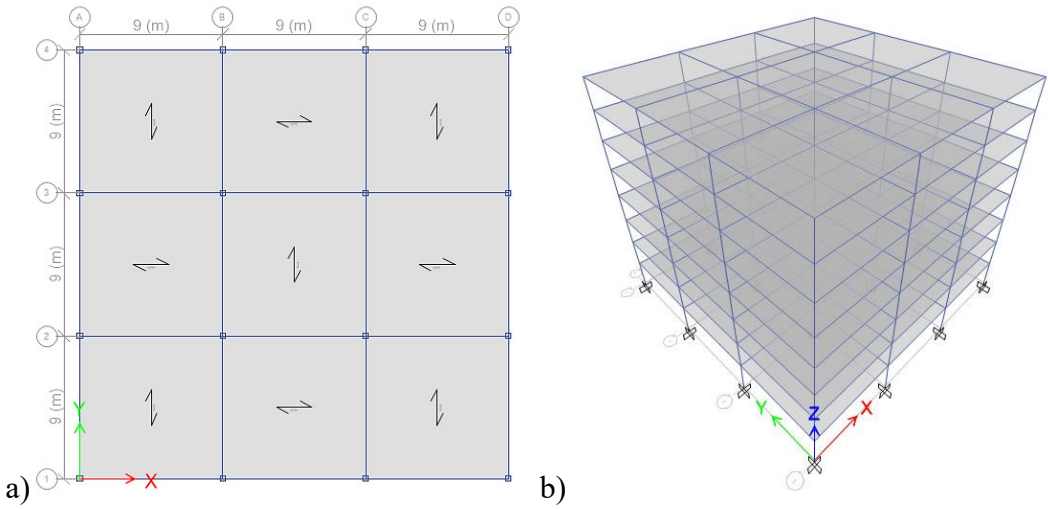

a) b)

Figure 4.3 a) Plan view of SMRF models; b) 3D view of 8-storey SMRF model

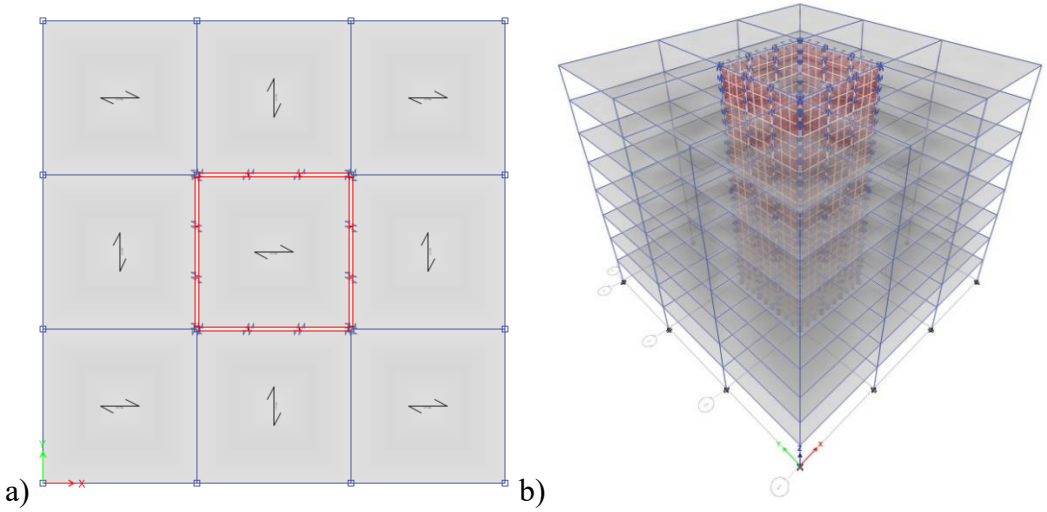

a) b)

Figure 4.4 a) Plan view of Hybrid model b) 3D view of 8-storey Hybrid model

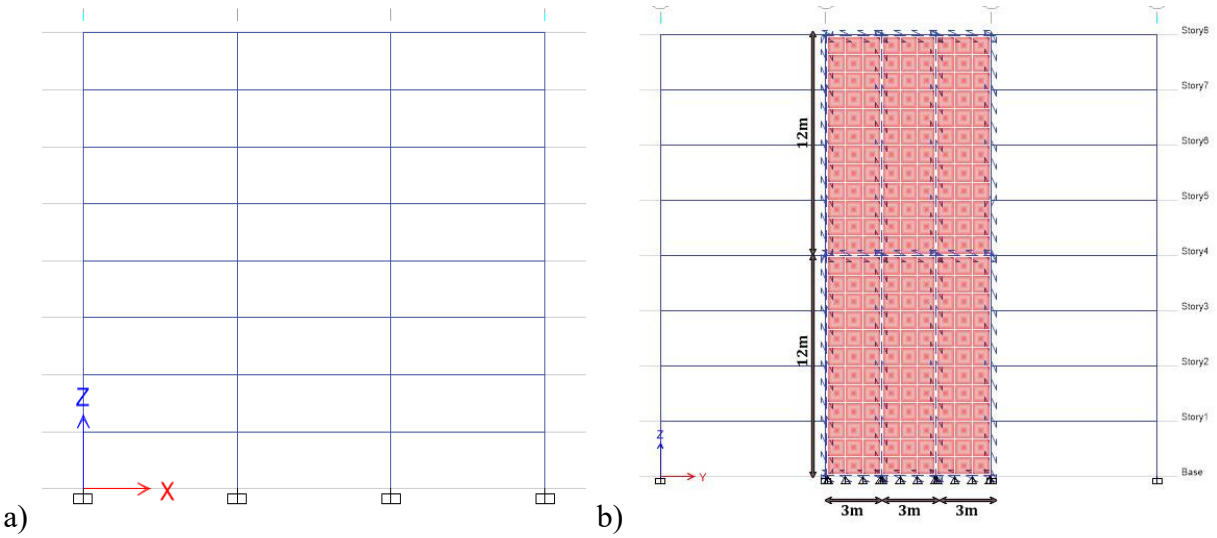

Figure 4.5 a) 8ST-HYBRID 2D model b) 8 ST-SMRF 2D model

Table 4.1 Overview of buildingmodels

Model Name	No. of Storeys	Lateral Resisting System
8-SMRF	8	Steel moderate ductile moment resisting frame (SMRF)
12-SMRF	12	
16-SMRF	16	
8-Hybrid	8	Hybrid MRF with CLT core shear walls (Hybrid)
12-Hybrid	12	
16-Hybrid	16	

4.3.1 Material Properties

The steel material properties used for modelling include 350 MPa yield stress (F_y), 200 GPa Elasticity modulus, and 0.01 strain hardening ratio. The CLT panels were modelled using orthotropic material and multi-layered shell elements. E1M5 grade was chosen with properties obtained from CSA O86 (2016), c.f. Table 4.2. Based on the findings from Connolly et al. (2018), 7-ply 245 mm thick CLT panels were employed.

Table 4.2 Material properties for CLT panels

Grain Direction	Ex (MPa)	Ey (MPa)	Ez (MPa)	Gxy (MPa)	Gyz (MPa)	Gzx (MPa)
Longitudinal Layers	11700	390	390	731	73.1	731
Transverse Layers	300	9000	300	563	563	56.3

4.3.2 Connections

The connection between the steel beams and columns is rigid; it could be welded or bolted. As for the connection between CLT panels, as well as the connection between CLT panels, steel columns, and the HDs to the foundation, the Holz-Stahl-Komposit (HSK™) (Bathon et al, 2014) connection was used, c.f. Figure 4.6. The steel holes are filled with an adhesive called adhesive dowels (AD), while the steel part between the two holes is called steel link (SL). This connection exhibits high stiffness and refrains ductility (Zhang et.al, 2018).

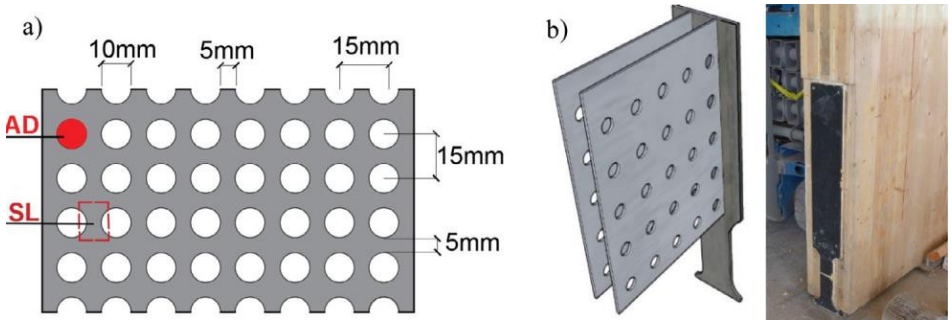

Figure 4.6 HSK connection: (a) Geometry; (b) Hold-down (Zhang et. al 2018)

Four types of HSK connections were employed in the model (Figure 4.7):

i) an HSK1 vertical connection (HSK1-V) used between the CLT panels;

ii) an HSK2 vertical connection (HSK2-V) used between panels and steel columns;

iii) an HSK2 horizontal connection (HSK2-H) used between CLT panels, and

iv) HLD used as hold-downs between CLT panels and foundation.

In specific, HSK1 is a short plate with 10 by 4 AD; HSK2 is the long plate consisting of 22 by 3.5 AD fitting in each side of CLT panels; and the HLD consist of two HSK plates with 22 by 8 AD each, along with steel tube and steel side plates connected to form a hold-down system. HSK1-V and HLD were designed to be dissipative connections. The HSK2V and HSK2H were designed as non-dissipative connections.

Each connection included tension and shear behaviour in two perpendicular directions. Figure 4.8 represents the shear and the tension behaviour for HSK 1 and HSK 2, along with the HLD uplift behaviour calculated and extracted from Zhang et al. (2018). In the modelling of these connections, vertical or horizontal placements altered their behaviour in each direction. In Table 4.3,**Error! Reference source not found.** connections and their material behaviour are illustrated in two orthogonal directions.

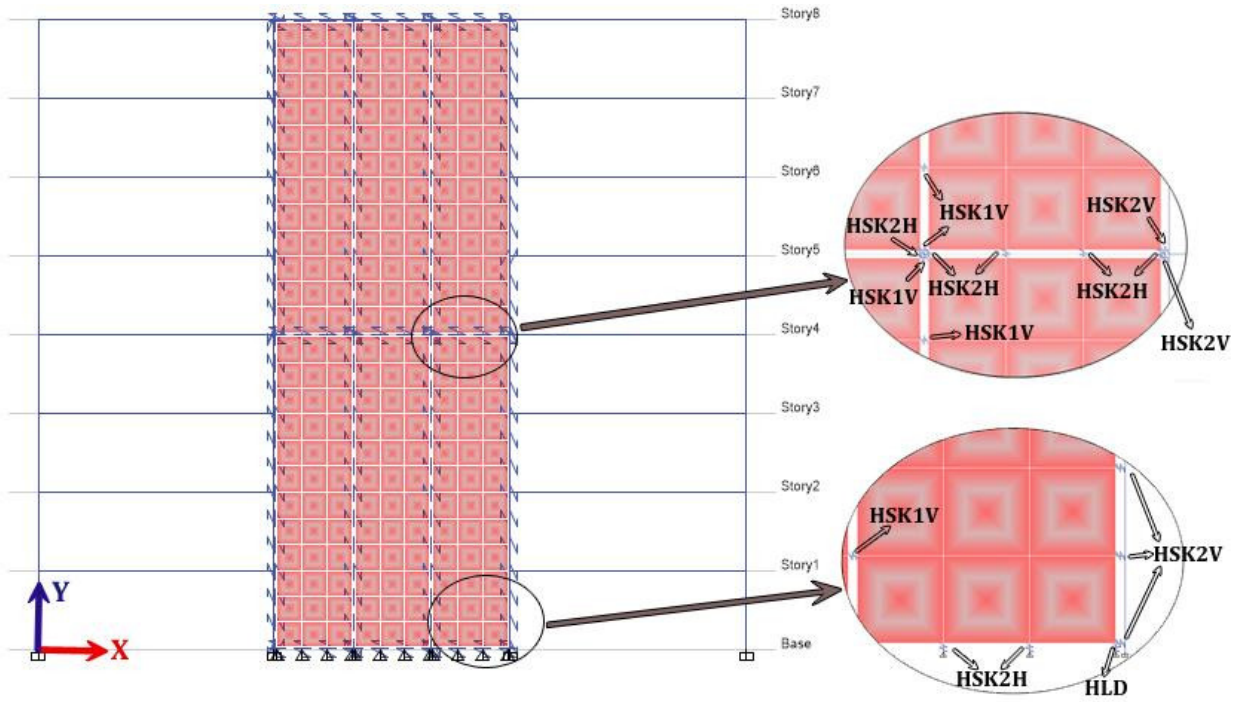

Figure 4.7 HSK Connection assignment to CLT panels and Columns

Table 4.3 Material Behaviour of HSK connections

HSK Connection	Material behaviour, X	Material behaviour, Y
HLD	-	HLD Uplift Behaviour (Figure 4.8 a)
HSK1V	HSK1-(Set up in Perp Layer of CLT) Tension Behaviour (Figure 4.8 c)	HSK1 Shear Behaviour (Figure 4.8 b)
HSK2V	HSK2-(Set up in Perp. Layer of CLT) Tension Behaviour (Figure 4.8 e)	HSK2 Shear Behaviour (Figure 4.8 d)
HSK2H	HSK2 Shear Behavior (Figure 4.8 d)	HSK2-(Set up in Par. Layer of CLT) Tension Behaviour (Figure 4.8 f)

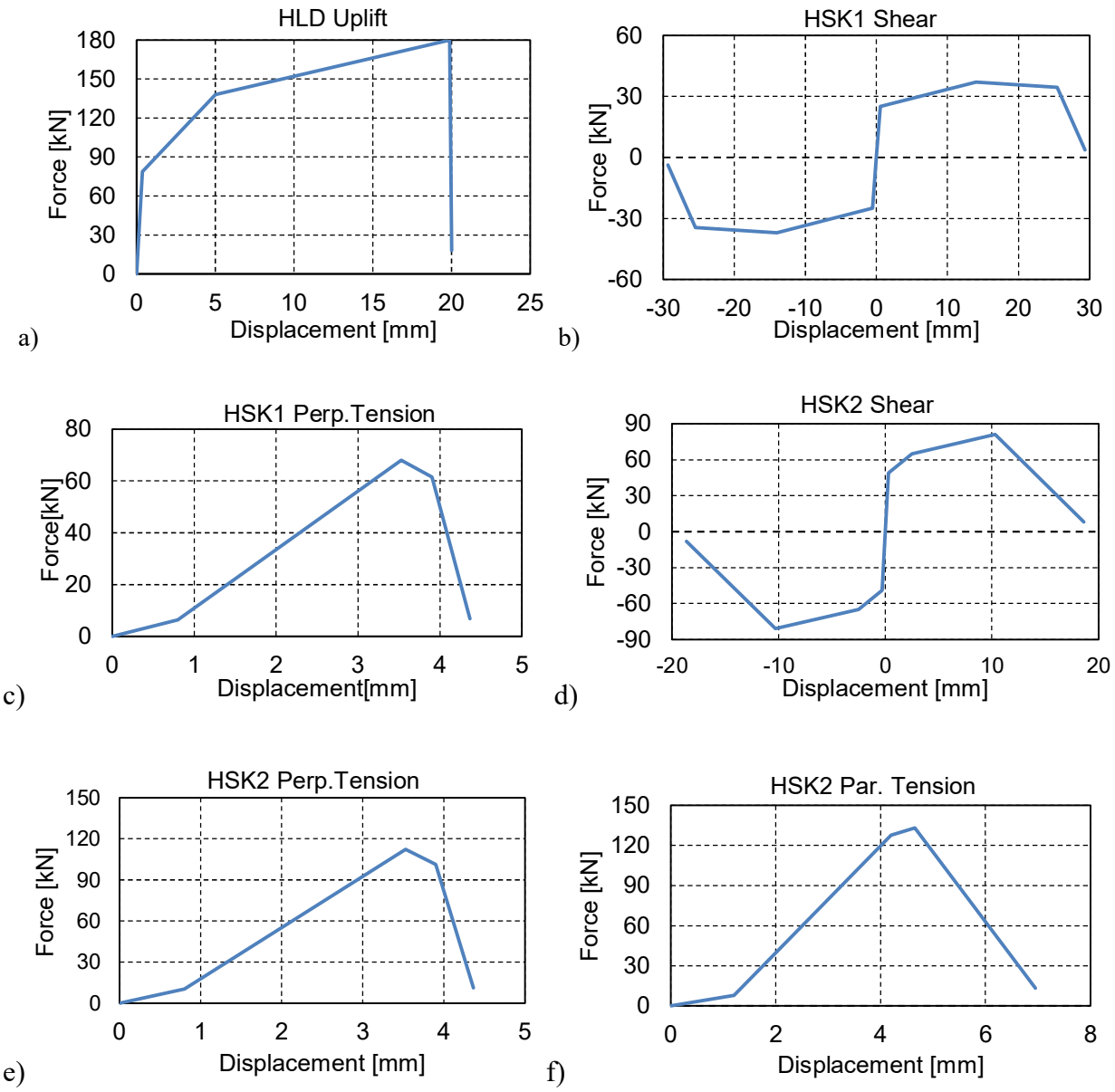

Figure 4.8 a) Hold-Down Uplift Behaviour; b) HSK1 Shear Behaviour; c) HSK1-(Set up in Perp Layer of CLT) Tension Behavior; d) HSK2 Shear Behavior; e) HSK2-(Set up in Perpendicular Layer of CLT) Tension Behavior; f) HSK2-(Set up in Parallel Layer of CLT) Tension Behavior

4.4 Loading

For all floors, partition and floor loads were added to the CLT panels. No partition load was applied to the roofs, resulting in a total dead load of 4.6 kN/m^2. Moreover, a snow load of 1.64 kN/m^2 was considered, and the live load was determined according to the NBCC (2015). Seismic parameters for the location of interest in Vancouver (City Hall) were obtained from NBCC, c.f. Table 4.4. The parameters define the horizontal spectrum acceleration, with 5% damping, and a 2% probability of being exceeded in 50 years. The acceleration spectrum is shown in Figure 4.10.

Table 4.4 Seismic Parameters

Location	S_a (0.2)	S_a (0.5)	S_a (1.0)	S_a (2.0)	S_a (5)	S_a (10)	PGA	PGV
Vancouver (City Hall)	0.848	0.751	0.425	0.257	0.08	0.029	0.369	0.553

In moderately-ductile moment-resisting frames, the ductility force modification factor (R_d) and the over-strength force modification factor (R_o) were obtained from NBCC (NBCC, 2015) as 3.5 and 1.5, respectively. It should be noted that balloon framing with CLT shear walls is not included in provisions provided by the NBCC. In this thesis, the calculation of the force modification factor for the Hybrid LLRS system (SMRF and CLT shear walls) will be investigated.

4.5 SMRF Preliminary Design

To design the initial cross-section for the members, 3D models for the SMRF were designed using MRSP analysis on ETABS in accordance with CSA-S16 (2014). According to NBCC 2015 Section 4.1.8.11-3, the fundamental lateral period for the steel moment-resisting frame and the Hybrid resisting system can be determined using equations 3.6 and 3.7.

As per NBCC (NBCC, 2015) section 4.1.8.11.3-d, for SMRF models, the empirical period may be multiplied by 1.5, while the obtained value shall not exceed the fundamental period obtained from

modal analysis. The minimum earthquake force (Table 4.5) is determined using equation 3.1 (NBCC 2015) and the value for S (T_a) is obtained from the acceleration spectrum. For moment-resisting frames and other systems in the present research such as the Hybrid system, V shall be greater than equation 3.3. Furthermore, in accordance with NBCC (NBCC, 2015) clause 4.1.8.12, the design base shear for the MRSP shall be scaled to 80% of ESFP base shear in the models.

Table 4.5 Seismic Base Shear for Strength Design Purpose of SMRF 3D models

Model	Height (m)	Empirical Period (Sec)	Modal Period (Sec)	S (Ta)	Eff. Weight (KN)	Base Shear (KN)
8ST-SMRF	24	0.92	2.16	0.361	29250	2010
12ST-SMRF	36	1.25	2.54	0.278	45855	2430
16ST-SMRF	48	1.55	3.01	0.257	61120	2992

According to NBCC (2015), to determine the deflections, V is allowed to be based on the value determined for T_a using modal analysis. However, the period shall be limited to 2.0 sec. In the SMRF model, the drift criteria govern the designs, even if the aforementioned modifications to the period are considered to determine base shear. To satisfy the drift criteria, all members' cross-sections are increased. By adding CLT shear walls to the Hybrid models and calculating the new seismic modification factor, the goal is to control the drift and optimize the design. The basic load combinations for the design is in accordance with NBCC (2015). The Design results for the 8-storey SMRF models are presented in Figure 4.9, while 12 and 16-storey models are shown in Appendix A. Also, the design of a sample cross section for a beam and a column is shown in Appendix A.

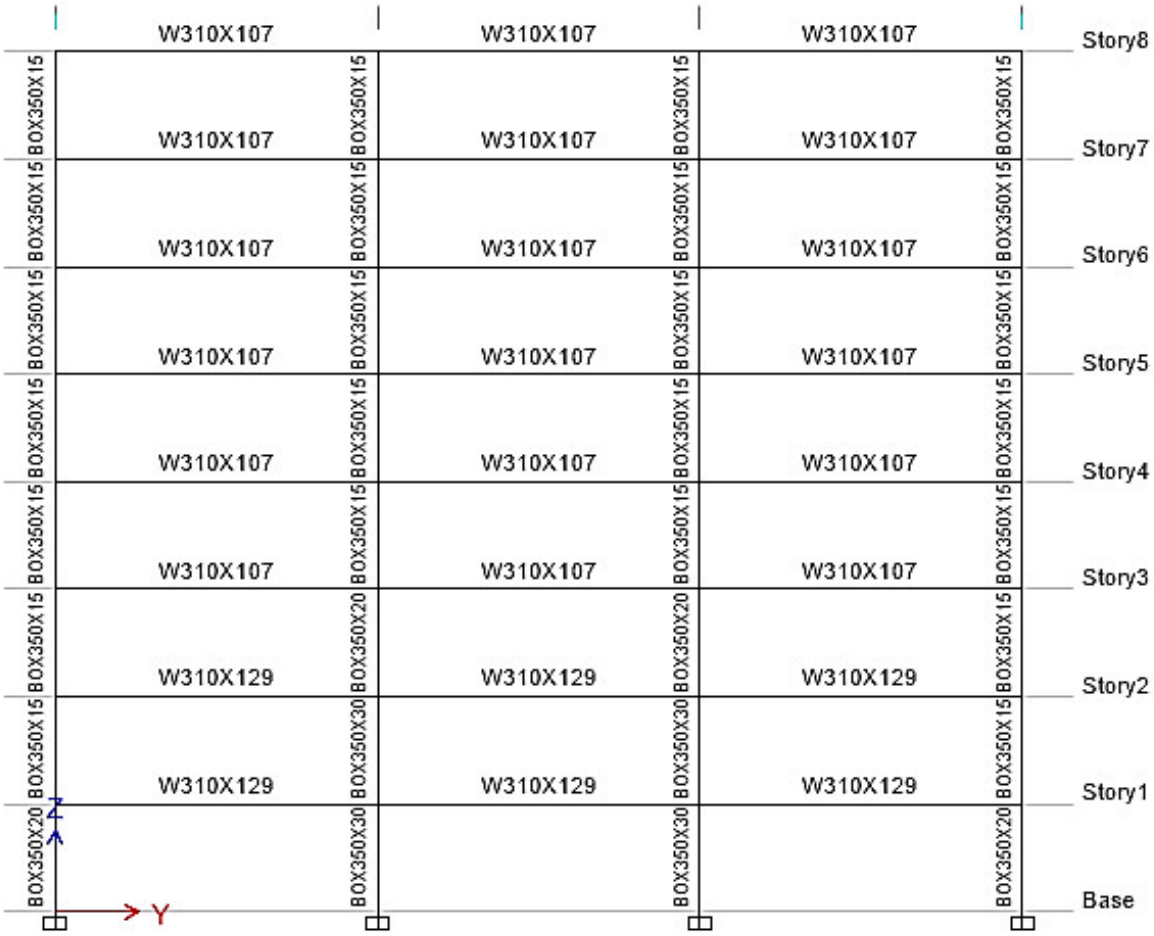

Figure 4.9 designed sections for middle frame of 8-storey SMRF model

4.6 Ground Motion Selection

To perform the NLTHA, appropriate acceleration records should be selected, which need to be scaled to the design spectrum as specified in the NBCC (2015). Ten records with horizontal component were selected and scaled to use for the time history analysis. For this purpose, the periods obtained from the modal analysis were used to determine the matching range with the NBCC design spectrum. First, the spectral amplitudes for the location in Vancouver (City Hall) were obtained from NBCC. The parameters define the horizontal spectral acceleration with 5% damping for seismic hazard, with a 2% probability of exceedance in 50 years, c.f. Figure 4.9. In accordance with ASCE 7 (2010), a period range between 0.2 T secs to 1.5 T secs was used to scale

the ground motions. The required ground motions were selected and scaled using the PEER NGA-WEST2 database (PEER, 2014). Figure 4.10 shows the acceleration spectra for the selected ground motions in relation to the NBCC design spectrum. Table 4.6 and Table 4.7 show the details and the scaling factors for the seismic records.

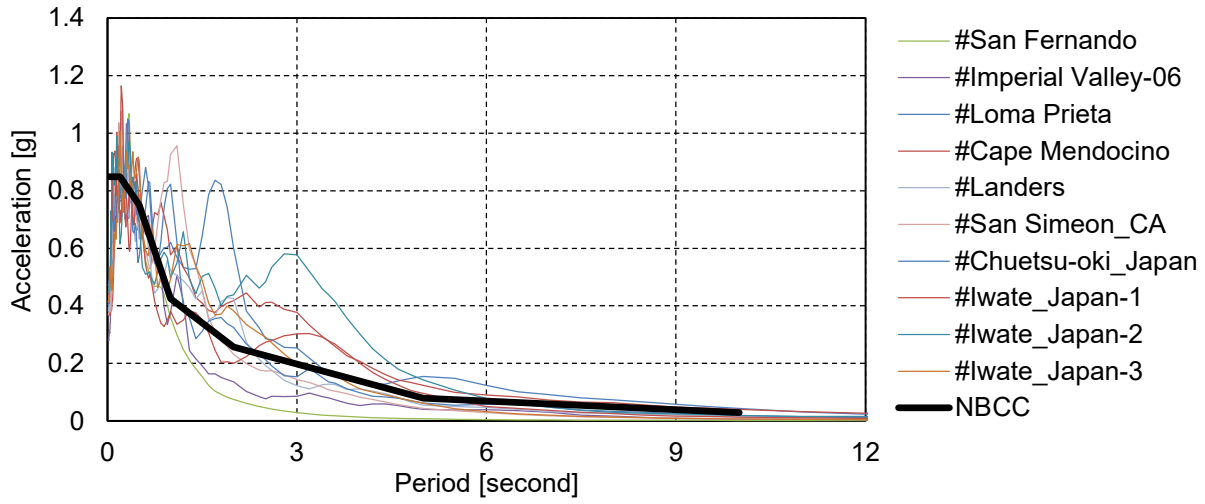

Figure 4.10 Details of selected acceleration records for time history analysis

Table 4.6 Details of Records

#	Earthquake Name	Year	Magnitude	Mechanism	Rjb* (km)	Rrup** (km)
57	San Fernando	1971	6.61	Reverse	19.3	22.6
164	Imperial Valley-06	1979	6.53	Strike slip	15.2	15.2
740	Loma Prieta	1989	6.93	Reverse Oblique	19.9	20.3
827	Cape Mendocino	1992	7.01	Reverse	16.0	20.0
3757	Landers	1992	7.28	Strike slip	26.9	26.9
4013	San Simeon_CA	2003	6.52	Reverse	16.2	19.0
5284	Chuetsu-oki_Japan	2007	6.8	Reverse	21.2	27.3
5776	Iwate_Japan-1	2008	6.9	Reverse	25.2	25.2
5800	Iwate_Japan-2	2008	6.9	Reverse	27.2	29.9
5806	Iwate_Japan-3	2008	6.9	Reverse	22.1	25.6

** RJB: Joyner-Boore distance: closest distance to the horizontal projection of the earthquake rupture plane (km)*

*** RRUP: Rupture distance: closest distance to the earthquake rupture plane (km)*

Table 4.7 Scale Factors of Records

#	Earthquake Name	8ST-Hybrid	12ST-Hybrid	16ST-Hybrid	8ST-SMRF	12ST-SMRF	16ST-SMRF
57	San Fernando	0.9446	0.9681	1.0774	1.5428	1.6871	1.8528
164	Imperial Valley-06	1.2128	1.1862	1.2522	1.5034	1.548	1.5639
740	Loma Prieta	3.8594	3.5116	3.0767	2.5138	2.4203	2.39
827	Cape Mendocino	2.2382	2.0257	1.9045	1.5026	1.4409	1.3868
3757	Landers	1.9471	1.8561	1.7956	1.7299	1.699	1.6872
4013	San Simeon_CA	2.4292	2.1131	2.0796	2.0087	1.978	1.9854
5284	Chuetsu-oki_Japan	2.0848	1.8932	1.8463	1.7687	1.7105	1.6858
5776	Iwate_Japan-1	2.017	2.1036	2.1217	1.9673	1.9097	1.8127
5800	Iwate_Japan-2	2.3292	2.2024	2.019	1.6119	1.5182	1.4141
5806	Iwate_Japan-3	1.3311	1.1963	1.1404	1.0151	0.9969	0.9832

4.7 Numerical Modelling

To perform modal, pushover and time history analyses, OpenSees (an open-source finite element method software for structural analysis) was employed (Mckenna, 2000). This software has an archive of material behaviours, steel, concrete, and various modelling elements. In addition to the elements in its archive, the user can define new material and elements for modelling. The software is capable of analyzing a variety of linear and nonlinear structural models.

2D models investigated (Figure 4.11). The beamWithHinges elements were employed to model the beam and columns and plastic hinges with Modified Ibarra-Medina-Krawinkler Deterioration Model with Bilinear Hysteretic Response (Ibarra et al, 2005. Lignos et al, 2011, Lignos 2008). To model the CLT shear wall panels, nDMaterial ElasticOrthotropic material and layered shell section (proposed by Lu et al, 2015)) were utilized. HSK connections were modelled using Pinching4 uniaxialMaterial (Mazzoni, 2006) and twoNodeLink elements (Schellenberg, 2014). Figure 4.12

and Figure 4.13 illustrate the modelling properties. The Pinching4 parameters for the connections are provided in Appendix E.

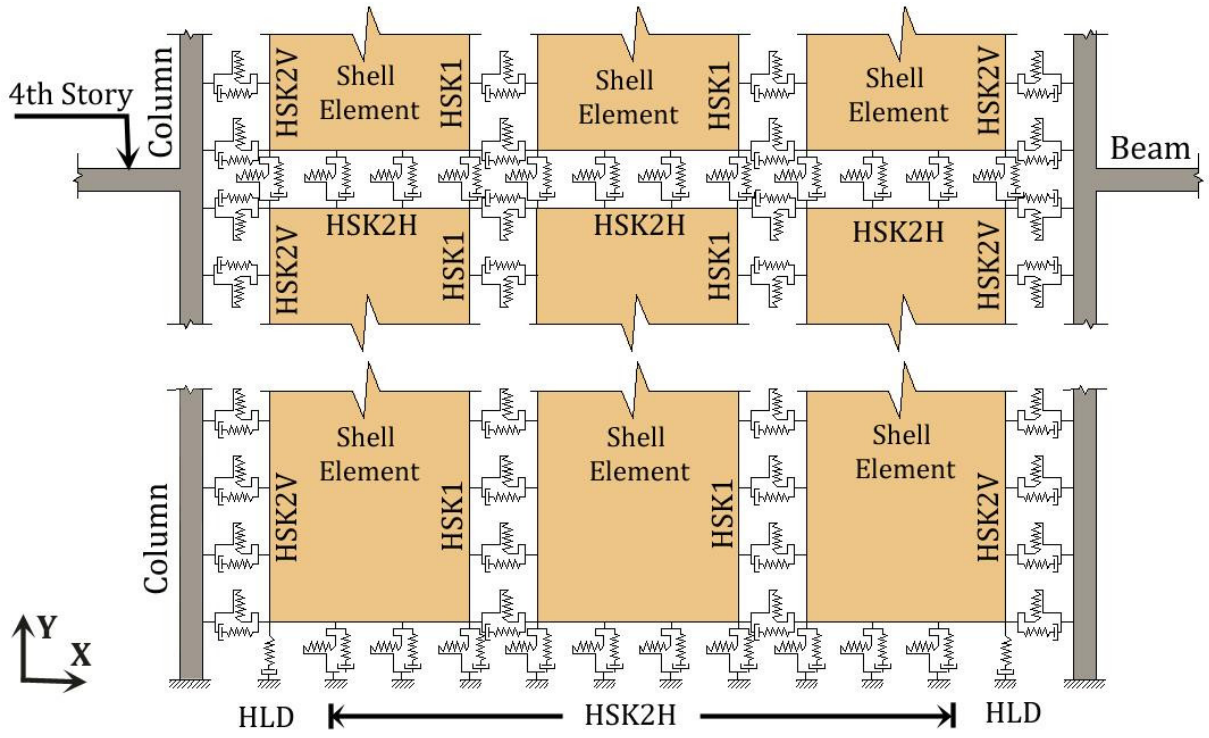

Figure 4.11 Numerical Model Schematic

The gap element (Mazzoni, 2006) is defined as the interacting element between CLT and the steel frame. This element is being used in addition to pinching4 to define the connection behaviours. If the HSK connections deform and fail, then the CLT panels come in contact with the steel frame. If there are no gap elements in the intersection points, the nods of the CLT panels in the model might pass the frame with no contact. Therefore, it is necessary to mode the gap element to account for the interaction between the CLT panels and the frame, along with the crushing of the CLT panels. Compression gap elements, with 20 mm gap distance, were used to constraint the CLT panels into the frames. Figure 4.14 shows the force-deformation behaviour of the gap elements. As can be

seen, after the gap zone, the CLT moves to an elastic zone defined according to its stiffness, followed by the yielding point, which can be determined by the CLT strength in compression.

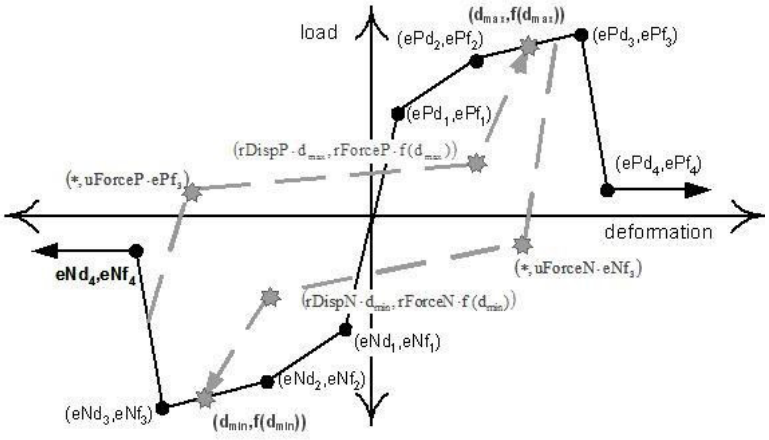

Figure 4.12 Pinching4 Material (Mazzoni, 2006)

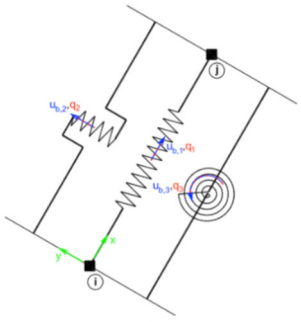

Figure 4.13 TwoNodeLink element (Schellenberg, 2014)

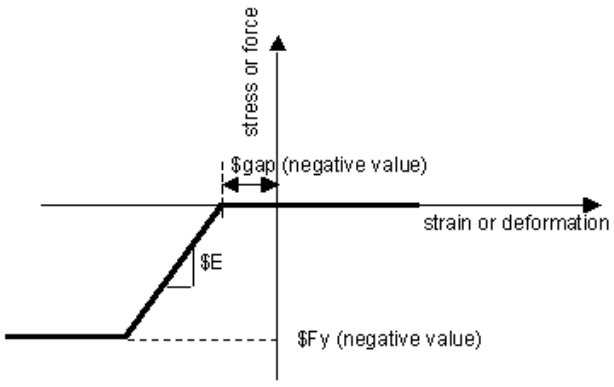

Figure 4.14 Compression gap element (Mazzoni, 2006)

The tension and shear behaviours of all HSK connections in the model were calibrated using the corresponding experimental tests by Zhang et al. (2018). The backbone curve of HSK connections were extracted from the experiments and then the backbone curves were equated to the 4-line curves (Figure 4.8). The comprehensive behaviour of the different HSK connections was defined based on their location and behaviour (Table 4.3). Using two node element and pinching4 material behaviour the HSK connections were modelled in Opensees.

Monotonic loading was applied to the connection models for calibrating tension behaviours of HSK. The CUREE testing protocol (Krawinkler et al, 2001) was used for calibration of cyclic shear behaviour of connections. The calibration results for HLD uplift behaviour, HSK1 and HSK2 shear behaviours are illustrated in **Error! Reference source not found.**, 4.16 and 4.17, respectively. The hold-down uplift experiment curve belongs to Monotonic Test 1, HSK1 shear behaviour for hysteretic curve for series 3-1(1)-Side A and HSK2 for Monotonic test Series 3-2 in Zhang et al. (2018).

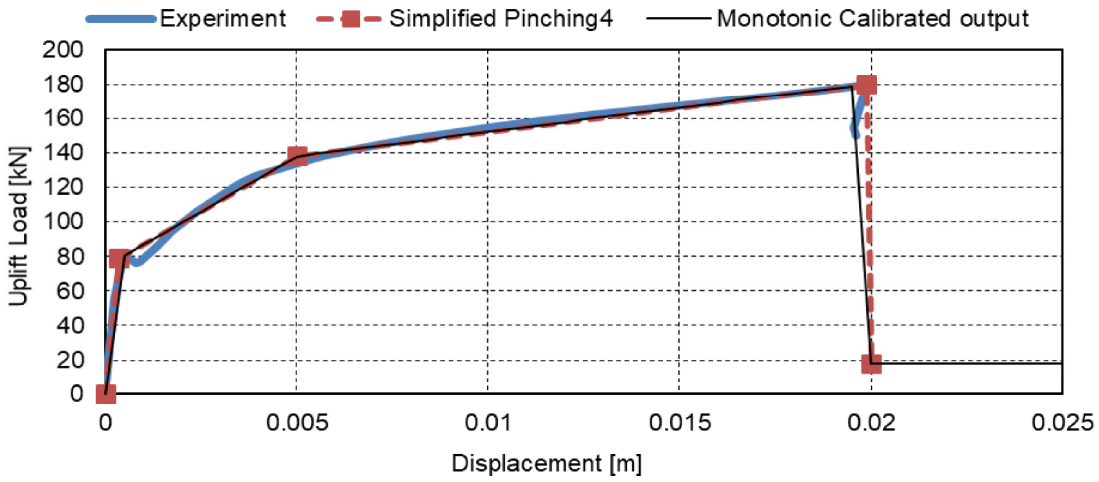

Figure 4.15 HLD uplift behaviour calibration [Zhang et al, 2018, hold down Monotonic Test 1]

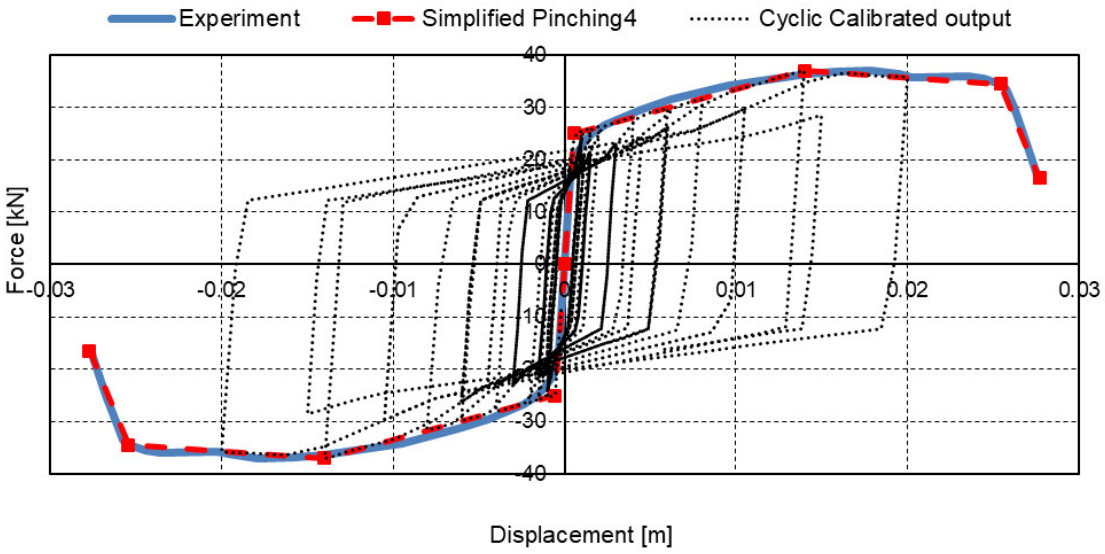

Figure 4.16 HSK1 Shear Behavior calibration, [Zhang et al 2018, Test S3-1]

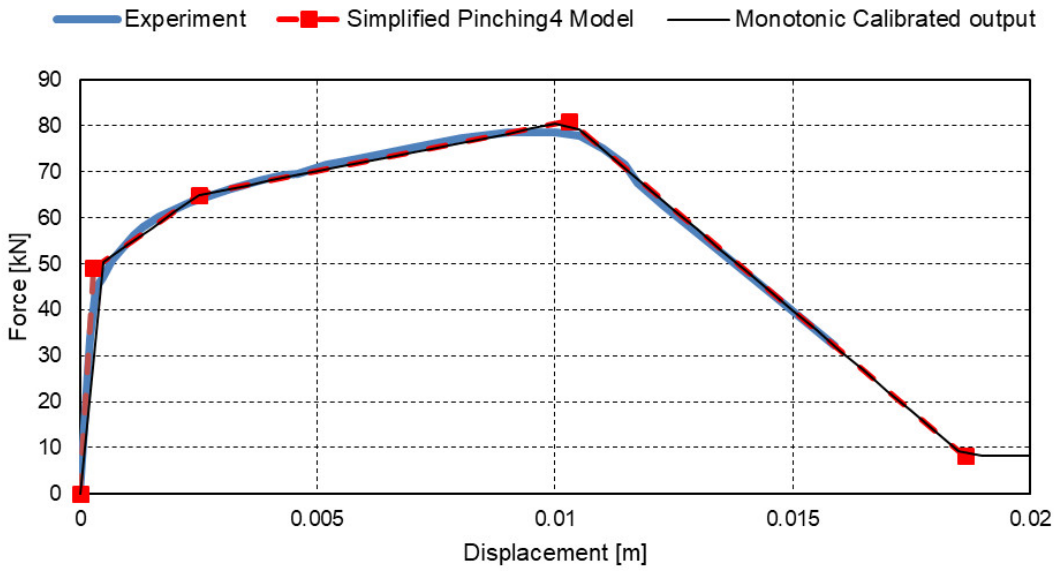

Figure 4.17 HSK2 Shear Behavior calibration, [Zhang et al 2018, Test S3-2]

5 Results

In this chapter, the results according to the analyses as shown in **Error! Reference source not found.** are presented. The outputs of modal analyses include periods of the first three modes of vibrations. The capacity curves of models obtained from push over analyses and the ductility and over-strength factors were derived from the push over outputs. Base shears, inter-storey drift and hold-down forces for both SMRF and Hybrid models are obtained and investigated from NLTHA.

5.1 Modal Analysis

Eigen value analysis was performed for all SMRF and HYBRID models with 8, 12, and 16 storeys in OpenSees and the period for the first three modes are given in Table 5.1. Table 5.1 compares the periods obtained from the NBCC and modal analyses. Comparing the empirical period computed based on NBCC (2015) provisions with the primary period of Hybrid models, it shows equation 3.7 can estimate the first mode period with sufficient accuracy for the 8-storey model. Figure 5.1**Error! Reference source not found.** shows the first mode periods of all models. In the HYBRID system, the periods are decreased by 73%, 62%, and 49% in the 8-, 12-, and 16-storey models, respectively. It proves that by adding CLT panels to SMRF, the system stiffness increased and this increase is lower for higher-level models. One reason for this difference is shear wall behaviour is mostly flexural for the high ratio of height to length of the wall and by rising its height its flexural stiffness decreased.

Table 5.1 Empirical Period and Period values obtained from modal analysis (seconds)

Period	8ST-SMRF	12ST-SMRF	16ST-SMRF	8ST-HYBRID	12ST-HYBRID	16ST-HYBRID
$T_{Empirical}$	0.92	1.24	1.55	0.54	0.74	0.91
Mode 1	2.03	2.26	2.37	0.55	0.87	1.20

Mode 2	0.65	0.78	0.85	0.17	0.27	0.38
Mode 3	0.36	0.46	0.49	0.10	0.15	0.21

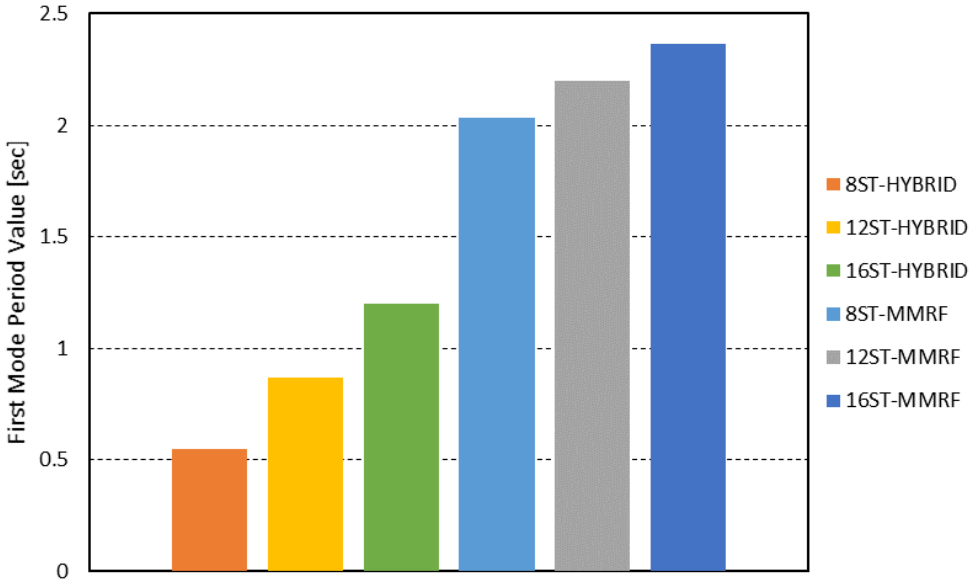

Figure 5.1 First Mode Period of SMRF and HYBRID Models

First mode shape of SMRF and HYBRID models are presented in Figure 5.2**Error! Reference source not found.**. The mode shapes are normalized for the sake of comparison. As it is clear, the first mode of SMRF models is similar to HYBRID models with a slight difference. This difference is the most for the 8-storey model and the least for the 16-storey model like the trend in the difference of the first period of models.

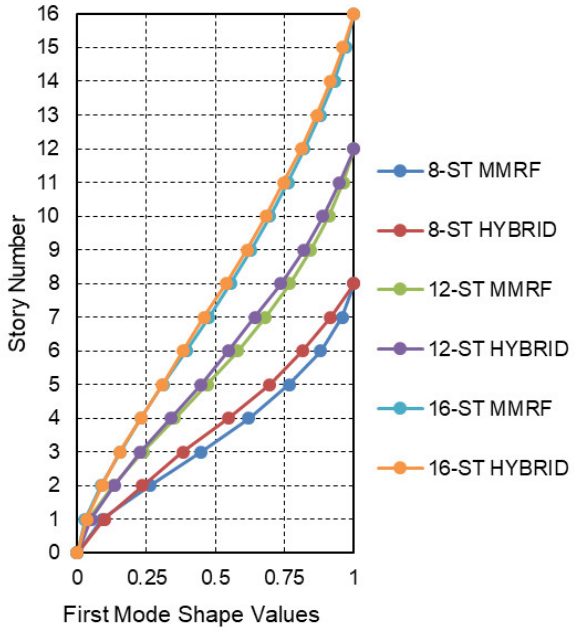

Figure 5.2 First Mode Shape of Models

5.2 Push-over analyses

5.2.1 Capacity Curves

The first mode from the modal analysis are used in Eq.3.10 and Eq.3.11 to calculate the yield displacement in push-over analysis. The capacity curve is the common output of pushover analysis which shows the base shear values vs. the roof displacement as a proxy for the nonlinear structural behaviour. Figure 5.3 shows the capacity curves for all 8-, 12-, and 16-storey Hybrid models. FEMA P695 provisions were used for calculating the target displacement, yielding base shear, yielding displacement, ductility factor and over strength factor. Target displacement corresponds to 80% of the maximum base shear experienced in the push-over analysis.

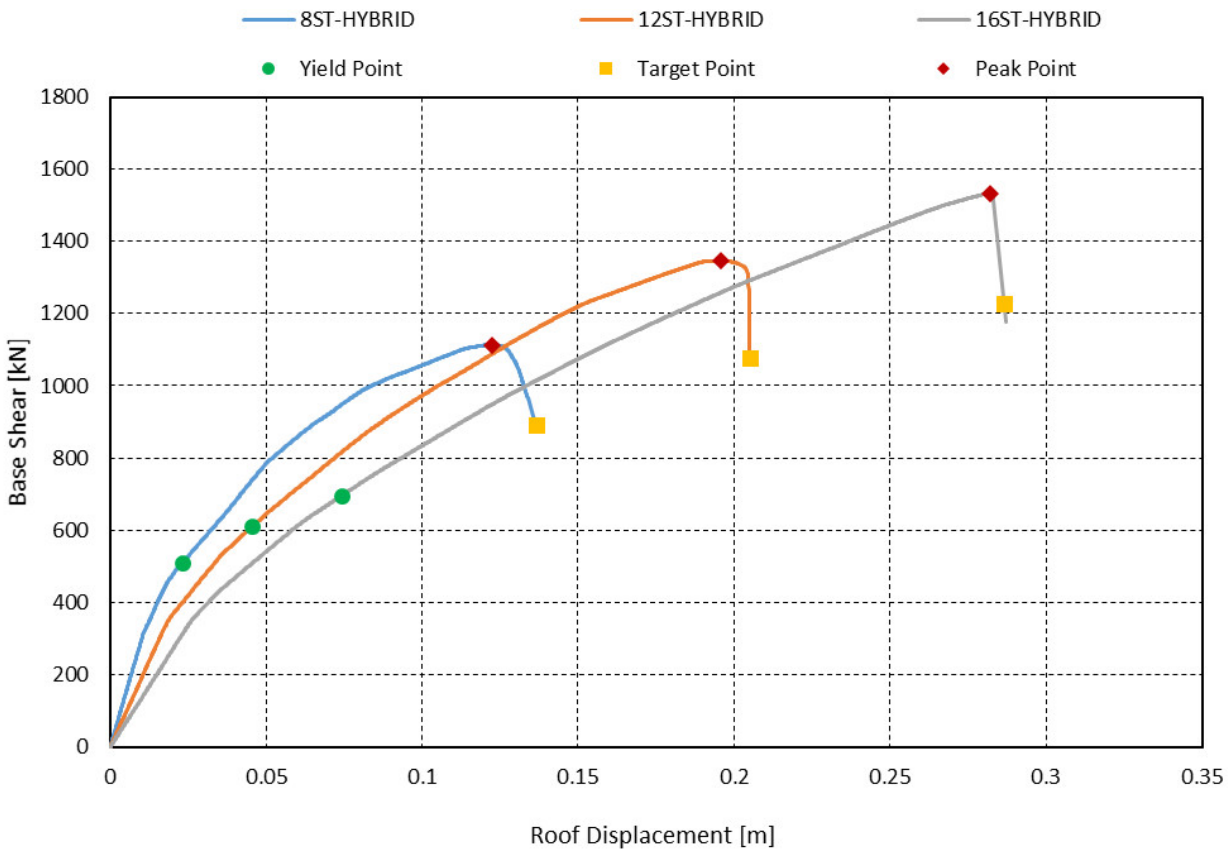

Figure 5.3 Capacity Curve for 8ST, 12 ST and 16ST- Hybrid Models

Table 5.2 summarizes the yield, peak and target points as obtained from the capacity curves for the 8-, 12- and 16-storey Hybrid models. All values increase with increasing building height with peak and target point increase almost proportional to building height. It is postulated that the target displacements for higher buildings can be estimated by linear extrapolation.

Table 5.2 Capacity Curve Coordinates

Point	Parameter	8ST-Hybrid	12ST-Hybrid	16ST-Hybrid
Yield Point	V_y (kN)	510	610	695
	$\delta_{y,eff}$ (mm)	23	46	74
Peak Point	V_{max} kN)	1,113	1,346	1,533
	δ_{Vmax} (mm)	122	196	282
Target Point	$0.8V_{max}$ (kN)	890	1,077	1,227
	δ_u (mm)	136	205	286

The ductility and overstrength factors were obtained using equations 3.7 and 3.8 and the parameters obtained from the capacity curve and the FEMA P695 procedure, c.f. Table 5.3.

Table 5.3 Parameters were obtained from pushover analysis to calculate μ and Ω

Model	δu (mm)	δy,eff (mm)	μ	Vmax (kN)	V (kN)	Ω
8ST-Hybrid	136	23	5.89	1,113	696	1.60
12ST-Hybrid	205	46	4.50	1,346	882	1.53
16ST-Hybrid	286	74	3.86	1,534	959	1.60

5.2.2 Seismic Performance Factors

The Newmark-Hall and Lai equations (Eq. 3.11 to 3.14) are used for obtaining the ductility reduction factor from the calculated ductility factor of the capacity curve reported in Table 5.4. The ductility reduction factors are obtained from Lai research are increased for the models with higher heights. This relation is not concluded from the Newmark-Hall 1982 formulation. The ductility reduction factor (Rμ). The average value of ductility reduction factors from the two aforementioned methods is 3.6 which can be compared with the value of Rd equal to 3.5 for moderately ductile steel moment resisting systems according to NBCC (2015).

Table 5.4 Ductility-based reduction factor

Models	Method	μ	Rμ
8ST-HYBRID	Newmark-Hall	5.89	3.55
	Lai	5.89	3.16
12ST-HYBRID	Newmark-Hall	4.50	4.06
	Lai	4.50	3.38
16ST-HYBRID	Newmark-Hall	3.86	3.86
	Lai	3.86	3.58

Table 5.5 shows the calculated over-strength and response modification factors for all models. The over-strength factors are similar and it can be postulated that further increasing the building height should not cause a significant change in over-strength factor. The average value of 1.57 can be an approximation of the NBCC Ro factors for the proposed hybrid system. (According to NBCC, the Ro factor for SMRF is 1.5.)

The average R factors according to the Newmark and Lai methods are 6.0 and 5.3, respectively and the overall average is 5.6 which can represent the response modification factor for hybrid steel moment resisting frame with balloon framing CLT shear walls system. According to NBCC, the R_dR_o for steel moment resisting frame is 5.25. Therefore, by adding the CLT balloon-farmed shear walls to create a hybrid system, the response modification factor, R in ASCE-7 or R_dR_o in NBCC is 5.6. This potential increase in the R factor means that the design base shear can be decreased, leading to smaller cross sections in design just to meet the force demands. But more importantly, adding CLT walls increases the system stiffness which leads to a more efficient design.

Table 5.5 Over-strength factors and response modification factors

Model	8ST-Hybrid	12ST-Hybrid	16ST-Hybrid	Average
Ω	1.60	1.53	1.60	1.57
R, (Newmark)	5.67	6.2	6.18	6.02
R, (Lai)	5.05	5.16	5.72	5.31

5.3 Time History Analyses Results

Nonlinear dynamic time history analyses (NLTHA) were conducted for the six Hybrid and SMRF models under the ten selected ground motions. For the comparison of system behaviour, the deformations, internal forces, and reaction forces were monitored and the inter-storey drift values, hold-downs uplift force and also the base shears under the ten ground motions were investigated.

5.3.1 Base Shear

The average of the maximum base shears obtained from the ten ground motions for each model is illustrated in Figure 5.4. The individual base shear forces are provided in Table 5.6 and illustrated in Appendix B.

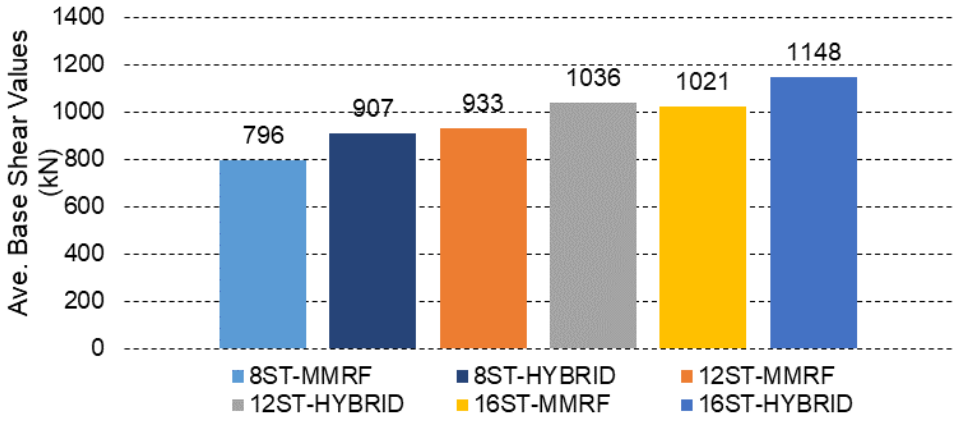

Figure 5.4 Base shear from NLTHA (average of 10 ground motions)

Table 5.6 Base shear from NLTHA of 10 ground motions

Ground motion	8ST-SMRF	8ST-Hybrid	12ST-SMRF	12ST-Hybrid	16ST-SMRF	16ST-Hybrid
Cape Mendocino000	905	1110	1128	1401	1308	1517
ImperialValley147	612	404	574	534	708	833
Iwate-KamiNS	790	798	967	1044	1002	1136
Iwate-YokoteNS	945	1155	1297	1400	1274	1223
IwateYuzawaNS	860	833	1036	967	1143	1147
Landers090	951	1015	1017	995	1040	1264
LomaPerieta250	959	1346	1076	1431	1121	1500
Nigh11NS	877	941	1061	975	1062	1149
SanFernando021	468	518	521	774	575	746
SanSimeon021	592	951	653	843	979	960
Average	796	907	933	1036	1021	1148

In the Hybrid models, base shear increased. But here it must be noted that the cross-sections going from the SMRF to the Hybrid were not optimised by remained the same. The CLT shear walls were added to the existing SMRF model and increased its stiffness and weight, and consequently, the base shear is slightly larger.

5.3.2 Inter-Storey Drift

For investigating the drift values, the maximum inter-storey drift for each storey during the NLTHA was recorded, see Figure 5.5. The lower buildings experienced higher drift values due to smaller frame cross-sections. Hybrid models in comparison to the SMRF models exhibited lower inter-storey drifts by a ratio of 2.8, 2.3, and 2.5 for 8-, 12-, and 16-storey models, respectively. The inter-storey drift for all Hybrid models with different building height is similar which shows that the CLT shear walls have been effective in all heights.

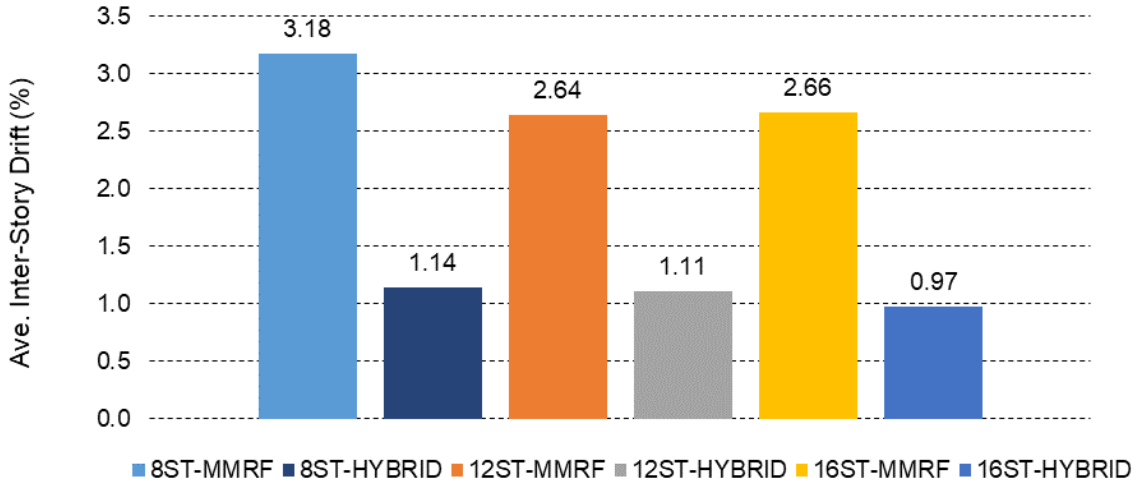

Figure 5.5 Average maximum inter-storey drift for all Models under ten ground motions

Figure 5.6 shows the averaged inter-storey drift distribution over the building height under the ten ground motions and compares them to the allowable drift according to the NBCC (2015). The drift

outputs in Hybrid models show smaller differences between storeys. In the 8 story SMRF model, the drift exceeded the NBCC allowable criterion, but in the 12 and 16 storey models, the drifts stayed within the allowable limit. The distribution of maximum inter-storey drift for all models under ten ground motions are shown in Table 5.7 and Appendix C.

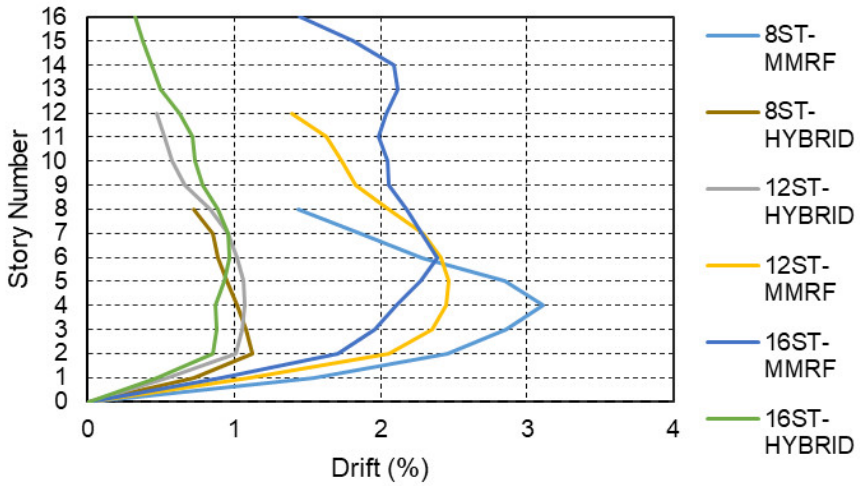

Figure 5.6 Average inter-storey drift distribution over the height of SMRF and HYBRID models

Table 5.7 Inter-Storey drift distribution for ten records

Ground Motion	8ST-SMRF	8ST-Hybrid	12ST-SMRF	12ST-Hybrid	16ST-SMRF	16ST-Hybrid
Cape Mendocino000	0.0409	0.0141	0.0333	0.0151	0.0336	0.0177
ImperialValley147	0.0155	0.0034	0.0145	0.0033	0.0147	0.0040
Iwate-KamiNS	0.0228	0.0083	0.0185	0.0092	0.0205	0.0094
Iwate-YokoteNS	0.0386	0.0154	0.0421	0.0176	0.0498	0.0088
IwateYuzawaNS	0.0330	0.0109	0.0321	0.0094	0.0247	0.0091
Landers090	0.0443	0.0123	0.0348	0.0104	0.0245	0.0123
LomaPerieta250	0.0600	0.0235	0.0354	0.0245	0.0328	0.0206
Nigh11NS	0.0273	0.0113	0.0277	0.0089	0.0225	0.0077
SanFernando021	0.0123	0.0040	0.0102	0.0043	0.0162	0.0045
SanSimeon021	0.0230	0.0105	0.0157	0.0082	0.0270	0.0072
Average	0.0318	0.0114	0.0264	0.0111	0.0266	0.0097

5.3.3 Hold-Down Forces

The average values of maximum uplift in the hold-down are shown in Figure 5.7. Increasing the building height increased the demand uplift force (twofold for the 16-storey models). The values of maximum forces in HLD under ten ground motions are shown in Table 5.8 and Appendix D.

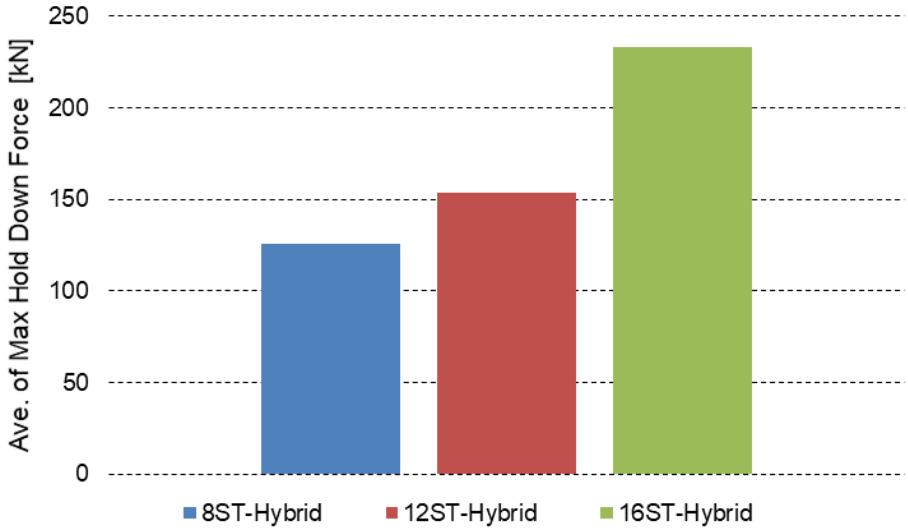

Figure 5.7 Average values of maximum tension forces in HLD1 under ten ground motions

Table 5.8 Maximum hold down uplift force in HLD1 under ten ground motion [kN]

Ground Motion / Model	8ST-Hybrid	12ST-Hybrid	16ST-Hybrid
Cape Mendocino000	135	174	302
ImperialValley147	93	98	189
Iwate-KamiNS	106	145	211
Iwate-YokoteNS	139	180	231
IwateYuzawaNS	134	165	224
Landers090	141	169	239
LomaPerieta250	180	180	302
Nigh11NS	108	155	215
SanFernando021	97	114	201
SanSimeon021	126	157	221
Average	126	154	234

5.4 Design of Hybrid Models

The Hybrid buildings were re-designed in Etabs using the reduction factors proposed in chapter 5.2. Seismic base shear for Hybrid 3D models are shown in Table 5.9 and the resulting steel reduction after designing according to CSA-S16 (2014) are listed in Table 5.10.

Table 5.9 Seismic Base Shear for Strength Design Purpose of Hybrid 3D models

Model	Height (m)	Empirical Period (Sec)	Modal Period (Sec)	S (Ta)	Eff. Weight (kN)	Base Shear (KN)
8ST-Hybrid	24	0.54	0.73	0.601	28,811	3,298
12ST- Hybrid	36	0.74	1.30	0.408	45,167	3,509
16ST-Hybrid	48	0.91	1.76	0.363	60,203	4,165

Table 5.10 Reduction of Steel Weight in Hybrid Models

Weight (Ton)	8ST-Hybrid	8ST-SMRF	Reduction (%)	12ST-Hybrid	12ST-SMRF	Reduction (%)	16ST-Hybrid	16ST-SMRF	Reduction (%)
Beams	145	254.3	**43**	279.5	446.7	**37**	289.9	613.9	**53**
Columns	68	65.3	**-4**	90.4	131.5	**31**	139.5	249.4	**44**
Total	214	319.7	**33**	370.0	578.3	**36**	429.4	863.4	**50**

It was possible to reduce the volume of steel in the Hybrid structures significantly compared to the SMRF structures. This reduction increased was 33, 36 and 50% for the 8-, 12- and 16-storey buildings, respectively. In the SMRF models to satisfy the NBCC drift criterion, bigger cross sections were needed. By adding CLT shear walls, the base shear was distributed between two LLRS and the resulting reduction of stresses within the SMRF helped that drift no longer governed the design; a better and more efficient structure was possible.

5.5 Discussion

A comparison between the ductility reported in Table 5.3 shows that Hybrid systems for 8-storey buildings could reach higher ductility by 52 and 30% compared to the 12 and 16-storey structures.

This indicates that the hybridisation is more efficient from a ductility perspective for lower structures. However, the resulting ductility-based reduction factors for all the Hybrid buildings are similar, showing that the hybridisation is a promising alternative for any building height. The over strength factor for all investigated building heights are very similar (1.57) and also similar to those accepted for pure SMRF structures (1.5).

As shown in Figure 5.3 , there is a relatively sudden degradation in the capacity curves of the models. This degradation is caused by the failure in one of the connections. It should be noted that the capacity curve was plotted just up to the target displacement point because the estimation of R factor was the goal. Model convergence was difficult due to micro modeling and number of nonlinear link elements. After this degradation, a hardening would be expected again in the curve as the steel frame intervenes in tolerating the lateral load. The current capacity curve is based on the current specific assumptions and models. By increasing the capacity of HSK connections, a higher capacity and smoother push-over curves would be expected.

The proposed R factor of 5.67 is an approximation based on the specific parameters used in the models. More accurate seismic modification factors must be calculated with Incremental Dynamic Analysis (IDA) following the FEMA P695 procedure. Further modeling would be required before an R factor for this hybrid system can be proposed for codes adoption. But based on the research presented herein, there is strong evidence that an R factor in the range of SMRF can be achieved by hybridization and that the NBCC approach of suing the lower R factor between the two systems, herein 1.3 for balloon-frames CLT shear walls is overly conservative and would lead to inefficient design. Another important finding is that even by considering an R factor less than 5.67 for the hybrid structure, the added CLT shearwalls will reduce the drift, and lead to reduction in the

volume of steel and a more efficient design compared to pure SMRF structures. This provides engineers and designers a good alternative.

The NLTHA showed that base shear increased for all Hybrid systems compared to the pure SMRF structures. In addition to the larger mass caused by simply adding shear walls to the existing design leading to lower first mode of vibration, this could be caused by the nature of the selected ground motions records. Using taller buildings with another series of ground motion, for instance far-fault ground motions, could change the results, i.e. lower base shear for taller buildings. Again, IDA would provide more comprehensive results.

One goal of current research was to reduce the drift criteria of SMRF structure. When designing SMRF structures, drifts criteria govern the design and not the strength criteria. Designers must size of members in SMRF to satisfy the drift while there is no problem with the strength of building or members. The drift ratios substantially decreased using the Hybrid models, due to the added stiffness from CLT panels. This is beneficial and compared to using steel braces and thin steel shear walls, there is no risk of local and global buckling. In addition to lower drift values, it was shown in Figure 5.6 , that the drift distribution over the height is more uniform for Hybrid systems, indicating a better “stiffness distribution” over the height of the structures. This reduces the inherent “soft story” nature of SMRF.

An important point to remember is that the SMRF models were designed so their drifts met the NBCC limits to be below 2.5%. Then, the CLT shear walls were added to the models and as a result, the maximum drift in hybrid models was significantly less than SMRF drift. This hybrid structure that was then analysed under nonlinear static and dynamic analysis is not the optimum design since its members are same as SMRF models for the sake of comparison. In practise, by adding the CLT, it is possible to reduce the size of steel members in the hybrid model which

reduces its stiffness, increase its ductility and leads to higher drifts in the Hybrid structure. As a consequence, the pushover curve would be different, too.

In chapter 5.4, the Hybrid structure was re-designed using the new proposed R factors. As can be seen in the Table 5.10, the weights of the Hybrid buildings were lower than that of SMRF, 50% reduction in steel material for 16-storey Hybrid structure and 33% reduction for the 8-storey structure. These lower weights along with eliminating some moment connections will reduce material usage and labor cost, resulting in overall cost. Additionally, the CLT panels with HSK connections are replaceable, making the structure more "resilient" for intense earthquakes. This comes to a higher importance for post-disaster structures which needs to be repaired and brought back to serviceability quickly.

Design base shear calculated by equivalent static procedure and response spectrum analysis of 3D Hybrid models also confirms the results of NLTH analysis. In hybrid systems reduction in main period of structure leads to higher acceleration ($S(T_a)$) in Vancouver response spectrum (Figure 4.10), on the other hand, the new proposed R factor has not increased significantly compared to SMRF structures in order to counteract the raise of acceleration. So the design base shear would be higher compared to SMRF as seen in Table 5.9. However, by using the dual LLRS system, the base shear is distributed between steel moment frame and CLT shear wall and has both systems carry lateral loads. Hence, more efficient designs with less volume of steel would result. The rate of reduction in beams are higher compared to columns and it is shown that beams have controlled the drift more than the columns in SMRF system. In 8-storey hybrid structure, the columns weight slightly increased compared to the other model's trend. This is because of the increase in the size of column adjacent to the shear wall. It is shown that the columns in low-rise SMRF has less

impression in controlling the drifts and by adding shear wall, the shear force interaction with columns has made an over stress on these columns and the size increased to control this effect.

6 Conclusions

6.1 Summary

One drawback in designing steel moment restaurant frame systems (SMRF) is their high lateral displacement that require large cross-sections to satisfy the drift criteria. Adding the CLT shear wall could be a good solution to improve the seismic performance of such structures. In this thesis, the seismic performances of a Hybrid steel wood structure with two lateral load resisting systems, namely SMRF and CLT balloon-framed shear walls, was evaluated and compared to a pure SMRF.

Modal analyses were performed. The results confirmed that the period of the first mode of frequency in Hybrid models was approximately equal to the empirical period recommended by the NBCC. When the CLT shear walls were added to the SMRF, they increased the lateral stiffness, which decreased the period significantly. In an 8-storey model, this reduction was more effective; increasing the height of the building decreased this reduction.

Push-over analyses was performed on the Hybrid models through the FEMA P-695 procedure. The results indicated that the combination of CLT shear walls with HSK connections presented a viable solution to improve the ductility and energy dissipation in the structure. An over-strength factor (R_o) of 1.57 and ductility reduction factor (R_d) of 3.6 were obtained for the Hybrid system resulting in an overall seismic response modification factor in the Hybrid models of $R_dR_o = 5.67$.

Nonlinear Time History analyses using ten earthquake records scaled to the Vancouver hazard spectrum were performed on both SMRF and Hybrid models. The CLT shear walls limited the lateral deformations, acting as a reinforcement of the steel frames. With the same member cross-sections, the demand base shear-induced in the Hybrid model was slightly higher than that of the SMRF models. The uplift force in the hold-down was driven and compared to each other under each record. For taller structures, the capacity of the hold-down should be increased for the design.

The Hybrid structures were redesigned using the new proposed response modification factors leading to a significant reduction in volume of steel usage. The concept of using an SMRF structure combined with CLT shear walls using HSK connections enhanced the structure's behaviour. Decreasing lateral displacements will decrease the steel material employed and increase the performance of the structure in earthquakes. Higher values in the response modification factor is a primary feature that confirms the consideration of this Hybrid system as a new LLRS in both new structures and retrofitting of weak structures.

6.2 Future Studies

For a comprehensive understanding regarding the behaviour of the current hybrid buildings with Hybrid LLRS system, the following future studies are recommended:

1. Numerical modeling of a different plan with different frames and a different CLT shear wall arrangement is required. A different location of the CLT in the plan, along with a different number of CLT panels in the bays could yield different results. More accurate modeling of the steel, CLT, and other components, along with 3-D modeling of the structure is necessary to see torsional effects and estimate a more realistic behaviour of the structure.
2. Comprehensive incremental dynamic analysis according to FEMA P-695 is needed to obtain a more accurate estimation of the seismic modification factors of this system.
3. The seismic performance and economical aspects of the current hybrid SMRF frames with CLT balloon framing type shear walls could be compared with similar structures with CLT platform construction infill wall to evaluate the feasibility and advantages of each structure.
4. Further studies on wind design, fire design, constructability, sound performance, and post-earthquake evaluation need to be conducted before such a system can be applied in practice.

Bibliography

ASCE7-10 (2010). “Minimum design loads for buildings and other structures.” American Society of Civil Engineers/Structural Engineering Institute (SEI) 7-10, Reston, Virginia, USA.

ASTM A992 / A992M-11(2015), “Standard Specification for Structural Steel Shapes”, ASTM International, West Conshohocken, PA, 2015, www.astm.org.

Bathon L., Bletz-Mühldorfer O., Schmidt J., Diehl Fatigue F., (2014). “Design of Adhesive Connections Using Perforated Steel Plates”, 13th World Conference for Timber Engineering, Quebec, CA.

Bezabeh M., Tesfamariam, S., Stiemer, S. (2015b). Equivalent Viscous Damping for Steel Moment-Resisting Frames with Cross-Laminated Timber Infill Walls. Journal of Structural Engineering. 04015080. 1-12. 10.1061/ (ASCE) ST.1943-541X.0001316.

Bezabeh, M., Tesfamariam, S., Stiemer S., Popovski M., Karacabeyli E. (2015a).”Direct Displacement Based Design of a Novel Hybrid Structure: Steel Moment-Resisting Frames with Cross Laminated Timber Infill Walls”. Earthquake Spectra. 32. 10.1193/101514EQS159M

Bhat P., (2013). “Experimental Investigation of Connection for the FFTT, A Timber-Steel Hybrid System”, MASc Thesis, University of British Columbia, Vancouver, Canada.

Ceccotti A., Follesa M., CNR-IVALASA. (2006a). “Seismic Behaviour of Multi-Storey X-Lam Buildings.” COST E29 International Workshop on Earthquake Engineering on Timber Structures, pages 81-95, Coimbra, Portugal.

Ceccotti A., Follesa M., Kawai N., Lauriola M.P., Minowa C., Sandhaas C., Yasumura M. (2006b). “Which Seismic Behaviour Factor for Multi-Storey Buildings made of Cross-Laminated Wooden Panels?” Proceedings of the 39th CIB W18 Meeting, paper 39-15-4.

Ceccotti, A. (2008). “New technologies for construction of medium-rise buildings in seismic regions: the XLAM case.” Structural Engineering International, 18(2), 156-165.

Ceccotti, A., Sandhaas, C., Okabe, M., Yasumura, M., Minowa, C., & Kawai, N. (2013). “SOFIE project–3D shaking table test on a seven-storey full-scale cross-laminated timber building.” Earthquake Engineering & Structural Dynamics, 42(13), 2003-2021.

Chok, K. (2004). “Lateral Systems for Tall Buildings.” Master's Thesis, Department of Civil and Environmental Engineering,, Massachusetts Institute of Technology. Massachusetts, USA

Computers and Structures Inc. (2013). “CSI analysis reference manual for SAP2000.” Berkeley, CA, USA.

Connolly, T., C. Loss, A. Iqbal and T. Tannert (2018). “Feasibility Study of Mass-Timber Cores for the UBC Tall Wood Building.” Buildings 8(8): 98. DOI: 10.3390/buildings8080098.

CSA O86-16 (2016). “Engineering design in wood.” Canadian standards association, Mississauga, ON.

CSA S16-14 (2014). “Design of Steel Structures 2014”, Canadian Standards Associations. Ottawa, Canada

CWC (2004). “Sustainability and life cycle Analysis for Residential Buildings”, Canadian Wood Council. International Building Series. No 4

CWC (2015). “Wood Innovation and Design Centre”. Canadian Wood Council. A technical case study report, Retrieved from http://wood-works.ca

Dickof, C., (2013). “CLT Infill Panels in Steel Moment Resisting Frames as a Hybrid Seismic Force Resisting System”, MASc Thesis, University of British Columbia, Vancouver, Canada.

Dickof, C. & Stiemer, S. & Bezabeh, Matiyas & Tesfamariam, Solomon. (2014). “CLT–Steel Hybrid System: Ductility and Overstrength Values Based on Static Pushover Analysis”. Journal of Performance of Constructed Facilities. 28. A4014012. 10.1061/ (ASCE) CF.1943-5509.0000614.

Dunn, A. (2015). “Final report for commercial building costing cases studies: traditional design versus timber project”. Melbourne, Australia: Forest and Wood Products Australia. [Report No. PNA308-1213].

FEMA. (2000). "Pre standard and Commentary for the Seismic Rehabilitation of Buildings." Rep. No. FEMA-356, Federal Emergency Management Agency, Washington, D.C.

FEMA. (2005). “Improvement of Nonlinear Static Seismic Analysis Procedures” Rep. No. FEMA-440, Federal Emergency Management Agency, Washington, D.C.

FEMA (2009) “Quantification of building seismic performance factors: FEMA P695” Federal Emergency Management Agency, Washington, D.C.

FII (2014) Forestry Innovation Investment and Binational softwood lumber council (BSLC),. “Summary Report: Survey of International Tall Wood Buildings” Report, May 2014, retrieved from: https://www.naturallywood.com

Green, M., & Karsh, E. (2012). “TALL WOOD: The Case for Tall Wood Buildings. How Mass Timber Offers a Safe, Economical, and Environmentally Friendly Alternative for Tall Building Structures” Vancouver, Canada

Ibarra, L.F., Medina, R.A. and Krawinkler, H. (2005). “Hysteretic models that incorporate strength and stiffness deterioration”. Earthquake Engineering and Structural Dynamics, 34, 1489-1511.

Janberg, N. (2003). “Alcoa Building, San Francisco, https://structurae.net”, image-id: 9358. Date taken: 28 May 2003.

Karacabeyli, E., Gagnon, S (2019). “Canadian CLT Handbook.” FPInnovations, 2019 edition, Volume 1 Vancouver, Canada.

Khorasani, Y. (2010). “Feasibility Study of Hybrid Wood Steel Structures” MASc Thesis, University of British Columbia, Vancouver, Canada

Koshihara, M., Isoda H., and S. Yusa. (2005). "The Design and Installation of Five-Storey New Timber Building in Japan." Summary of Technical Papers of Annual Meeting. Architectural Institute of Japan. 201-206.

Krawinkler, H., F. Parisi, L. Ibarra, A. Ayoub, and R. Medina. n.d. (2001) “Development of a Testing Protocol for Wood frame Structures.” CUREE Publication No. W-02, Consortium of Universities for Research in Earthquake Engineering.

Kremer, P. Symmons, M. (2015). “Mass timber construction as an alternative to concrete and steel in the Australia building industry: A PESTEL evaluation of the potential”. International Wood Products Journal. 6. 2042645315Y.000. 10.1179/2042645315Y.0000000010.

Lai, S.P. and Biggs, J.M. (1980). “Inelastic response spectra for aseismic building design", J. of the Struct. Div., 106(6), pp.1295-1310

Lignos, D.G., and Krawinkler, H. (2011) “Deterioration modelling of steel components in support of collapse prediction of steel moment frames under earthquake loading”, Journal of Structural Engineering, ASCE, Vol. 137 (11), 1291-1302. File:BilinMaterialOpenSees.pdf.

Lingos D.G., (2008)” sidesway collapse of deteriorating structural systems under seismic excitations” doctor of philosophy dissertation, department of civil and environmental, University of Stanford, California, US

Lu XZ, Xie LL, Guan H, Huang YL, Lu X,(2015) “A shear wall element for nonlinear seismic analysis of super-tall buildings using OpenSees”, Finite Elements in Analysis & Design, 2015, 98: 14-25.

Mazzoni S., McKenna F., Scott MH, Fenves GL, et al.(2006) “OpenSees Command Language Manual” Pacific Earthquake Engineering Research (PEER) Center, University of California, Berkeley, CA, <http://opensees.berkely.edu>.

McKenna F, Fenves GL, Scott MH. (2000). “Open system for earthquake engineering simulation.” University of California, Berkeley, CA, <http://opensees.berkely.edu>.

Miranda, E. and Bertero, V.V. (1994).”Evaluation of strength reduction factors for earthquake-resistant design", Earthquake Spectra, 10(2), pp. 357-379

Moehle, J. and Deierlein, G.G. (2004). A framework methodology for performance-based earthquake engineering. In: Proccedings of the 13th World Conference on Earthquake Engineering, Vancouver, B.C., Canada, August 1-6, 2004, Paper No. 679.

Mostafaei, Hossein; Al-Chatti, Qusay; Popovski, M; Tesfamariam, Solomon; Bénichou, Noureddine, (2013)” Seismic performance of wood mid-rise structures” Research Report No. RR-345 (National Research Council of Canada. Construction), 2013-09-24

NBCC (2015). “National Building Code of Canada 2015, Canadian Commission on Building and Fire Codes.” National Research Council of Canada, Ottawa, ON.

Newmark, N. M., and Hall, W. J. (1982). “Earthquake spectra and design”. Earthquake Eng. Res. Inst., El Cerrito, Calif.

NIST GSR 11-917-15. (2011).” Selecting and Scaling Earthquake Ground Motions for Performing Response-History Analyses” National Institute of standards and technology. US department of commerce.

NRC (2018),” Greening our built environments with wood” Natural Resource Canada, web report, retrieved from: https://www.nrcan.gc.ca [Accessed March, 2020]

PEER. (2014). Pacific Earthquake Engineering Research (PEER) NGA-West2 Database. 2014, Retrieved from https://ngawest2.berkeley.edu/

Popovski, M., Schneider, J., & Schweinsteiger, M. (2010). “Lateral Load Resistance of Cross-Laminated Wood Panels.” In World Conference on Timber Engineering (pp. 20-24).

Pei, S. and van de Lindt, J.W., (2007). “User’s Manual for SAPWood for Windows: Seismic Analysis Package for Woodframe Structures.” Colorado State University, Fort Collins, CO.USA

Pei, S., van de Lindt, J. W., & Popovski, M. (2013).” Approximate R-factor for cross-laminated timber walls in multistorey buildings”. Journal of Architectural Engineering, 19(4), 245-255.

Poirier, E.; Moudgil, M.; Fallahi, A.; Staub-French, S.; Tannert, T. “Design and construction of a 53 meter tall timber building at the university of British Columbia” World Conference on Timber Engineering (WCTE2016), Vienna, Austria, 22–25 August 2016.

Rethink wood. (2015), “designing for earthquakes. Wood is a proven choice for seismic-resistive construction” Content provided by the American Wood Council, Engineering News-Record. Retrieved from: http://www.woodworks.org

Schellenberg, A. (2014). “Two Node Link Element.” Opensees Wiki, University of California, Berkeley. Retrieved from: http://opensees.berkeley.edu

SOM (2013), “Timber Tower Research Project,” Skidmore Owings & Merrill. Final Report, Chicago, USA

Slavid, R. (2005) "Wood Architecture", London Laurence King Publishing Ltd, pp 239

United Nations. (2015) “World Population Prospects- The 2015 Revision,” Department of Economic and Social Affairs, New York, 2015.

Tesfamariam, S., Stiemer, S., Bezabeh, M., Goertz, C., Popovski, M., Goda, K. (2015). “Force based design guideline for timber-steel hybrid structures: steel moment resisting frames with CLT infill walls”. DOI: 10.14288/1.0223405.

Vamvatsikos, D. & Cornell, C.. (2002). Incremental Dynamic Analysis. Earthquake Engineering & Structural Dynamics. 31. 491 - 514. 10.1002/eqe.141.

Yasumura, M., Kobayashi, K., Okabe, M., Miyake, T., & Matsumoto, K. (2015). “Full-scale tests and numerical analysis of low-rise CLT structures under lateral loading.” Journal of Structural Engineering, 142(4), E4015007. DOI: 10.1061/ (ASCE) ST.1943-541X.0001348.

Yasumura, M (2000). “Dynamic analysis and modeling of wood-framed shear walls”, Proceedings 6th World Conference on Timber Engineering, Whistler, Canada, 2000

Zhang, X., Popovski M., Tannert T., (2018). “High-capacity hold-down for mass-timber buildings.” Construction and Building Materials. 164. 688-703.

Appendix A SMRF Frame Design

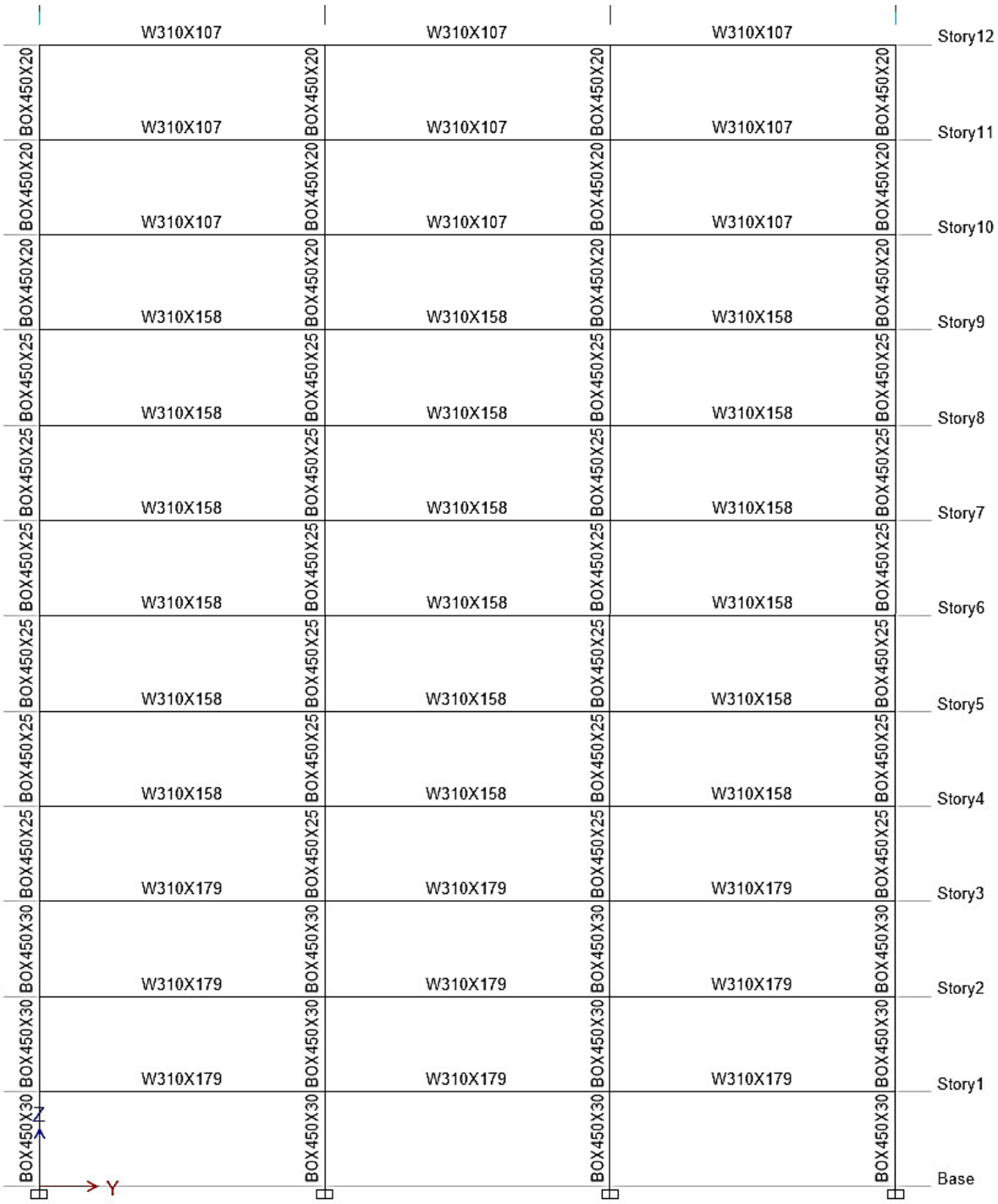

Figure A.1 Sections for middle frame of 12-storey SMRF model

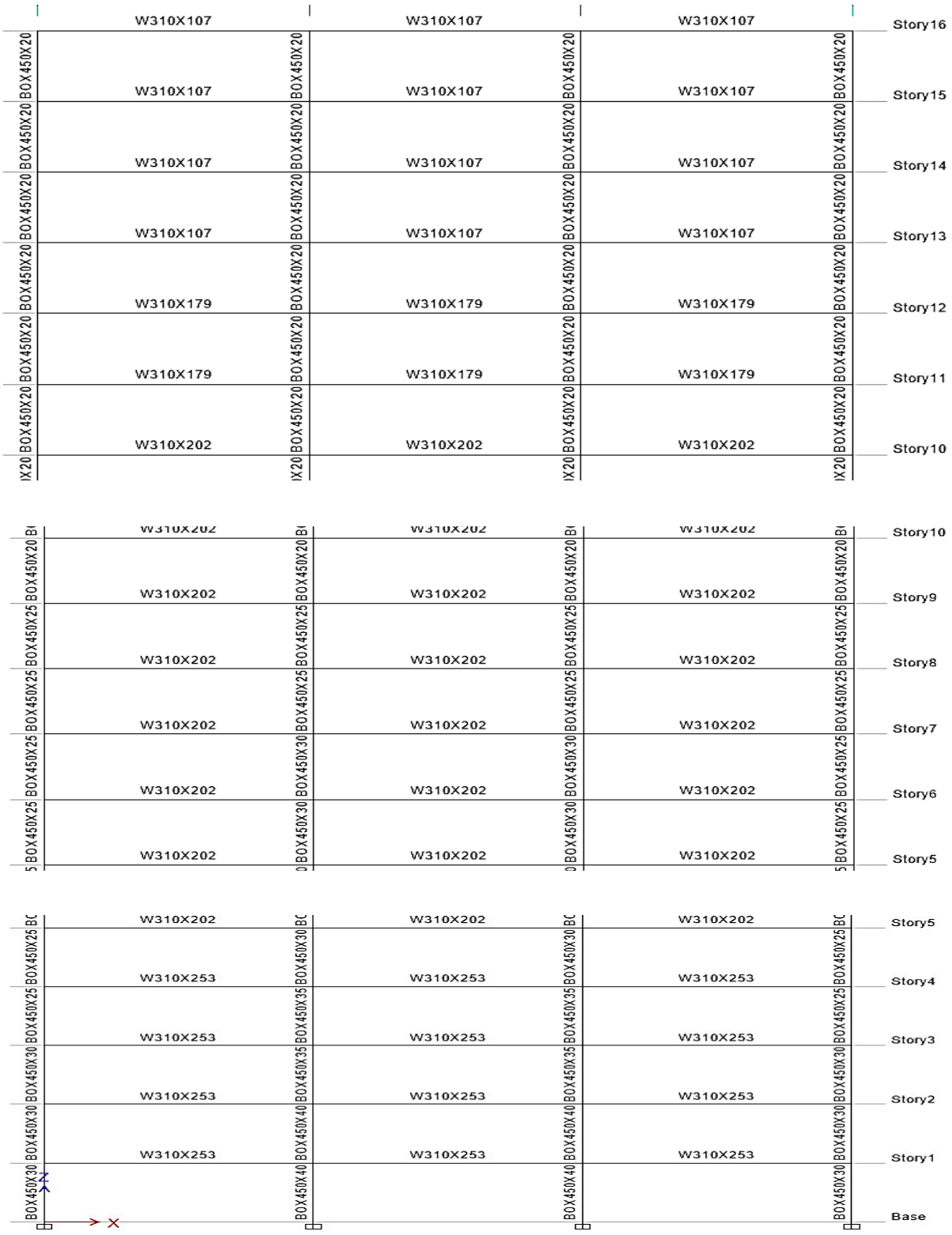

Figure A.2 Sections for middle frame of 16-storey SMRF model

Summary design of the highlighted Beam and Column in Figure A.3 of 8 Story SMRF building is described below:

Figure A.3 Highlighted beam and column for detailed summary design

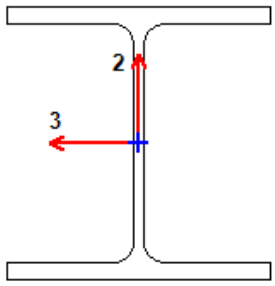

Element Details

Level	Element	Unique Name	Location (m)	Combo	Element Type	Section	Classification
Story1	B13	139	0.175	NBCC06	Type MD Moment Resisting Frame	W310X129	Class 1

Seismic Parameters (Part 1 of 2)

System R_d	System R_o	System Ie*Fa*Sa(0.2)	Slenderness Procedure	Ignore Seismic Code?
3.5	1.5	0.848	No	No

Seismic Parameters (Part 2 of 2)

Ignore Special Seismic Load?	Doubler Plate Plug Welded?
No	Yes

Design Code Parameters

Φ_b	Φ_c	Φ_t	Φ_v
0.9	0.9	0.9	0.9

Section Properties

A (m^2)	I_{33} (m^4)	r_{33} (m)	S_{33} (m^3)	A_{v3} (m^2)	Z_{33} (m^3)
0.0165	0.000308	0.13663	0.001937	0.0127	0.00216

J (m^4)	I_{22} (m^4)	r_{22} (m)	S_{22} (m^3)	A_{v2} (m^2)	Z_{22} (m^3)	C_w (m^6)
0.000002	0.0001	0.07785	0.000649	0.0042	0.000991	0

Material Properties

E (kN/m^2)	f_y (kN/m^2)	R_y	α
200000000	350000	1	NA

Demand/Capacity (D/C) Ratio (13.9b)

D/C Ratio	Axial Ratio	Flexural Ratio$_{Major}$	Flexural Ratio$_{Minor}$
0.707	0 +	0.708 +	3.6E-05

Stress Check Forces and Moments (13.9b) (Combo NBCC06)

Location (m)	P_f (kN)	M_{f33} (kN-m)	M_{f22} (kN-m)	V_{f2} (kN)	V_{f3} (kN)
0.175	5.9963	-469.639	0.0112	-273.8725	-0.005

Axial Force & Biaxial Moment Design Factors (13.9b)

	L Factor	K Factor	U_1	U_2	Ω_1	Ω_2
Major Bending	0.961	1	1	1	1	1.82
Minor Bending	0.01	1	1	1	1	

Axial Force and Capacities

P_f Force (kN)	C_r Resistance (kN)	T_r Resistance (kN)
5.9963	3604.8273	5197.5

Moments and Capacities

	M_f Moment (kN-m)	M_r Resistance (kN-m)
Major Bending	469.639	663.6374
Minor Bending	0.0112	312.165

Shear Design

	V_f Force (kN)	V_r Resistance (kN)	Stress Ratio
Major Shear	273.8725	866.0698	0.316
Minor Shear	0.005	2638.1678	0

End Reaction Major Shear Forces

Left End Reaction (kN)	Load Combo	Right End Reaction (kN)	Load Combo
-352.8793	NBCC35	342.8051	NBCC35

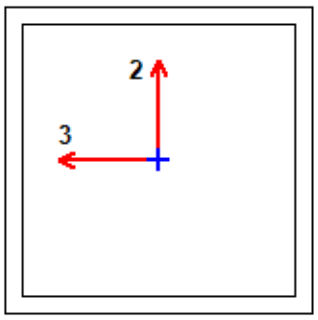

Element Details

Level	Element	Unique Name	Location (m)	Combo	Element Type	Section	Classification
Story1	C8	265	0	NBCC32	Type MD Moment Resisting Frame	BOX350X20	Class 1

Seismic Parameters (Part 1 of 2)

System R_d	System R_o	System Ie*Fa*Sa(0.2)	Slenderness Procedure	Ignore Seismic Code?
3.5	1.5	0.848	No	No

Seismic Parameters (Part 2 of 2)

Ignore Special Seismic Load?	Doubler Plate Plug Welded?
No	Yes

Design Code Parameters

Φ_b	Φ_c	Φ_t	Φ_v
0.9	0.9	0.9	0.9

Section Properties

A (m^2)	I_{33} (m^4)	r_{33} (m)	S_{33} (m^3)	A_{v3} (m^2)	Z_{33} (m^3)
0.0264	0.000481	0.13497	0.002748	0.0124	0.003271

J (m^4)	I_{22} (m^4)	r_{22} (m)	S_{22} (m^3)	A_{v2} (m^2)	Z_{22} (m^3)	C_w (m^6)
0.000719	0.000481	0.13497	0.002748	0.0124	0.003271	

Material Properties

E (kN/m^2)	f_y (kN/m^2)	R_y	α
200000000	350000	1.314	NA

Demand/Capacity (D/C) Ratio (13.8.3c)

D/C Ratio	Axial Ratio	Flexural Ratio$_{Major}$	Flexural Ratio$_{Minor}$
0.885	0.513 +	0.328 +	0.043

Stress Check Forces and Moments (13.8.3c) (Combo NBCC32)

Location (m)	P_f (kN)	M_{f33} (kN-m)	M_{f22} (kN-m)	V_{f2} (kN)	V_{f3} (kN)
0	-2133.8482	338.2684	-44.5768	162.151	-29.4275

Axial Force & Biaxial Moment Design Factors (13.8.3c)

	L Factor	K Factor	U_1	U_2	Ω_1	Ω_2
Major Bending	0.894	1.852	0.864	1	0.85	2.032
Minor Bending	0.894	1.646	0.864	1	0.85	

Axial Force and Capacities

P_f Force (kN)	C_r Resistance (kN)	T_r Resistance (kN)
2133.8482	4158	4158

Moments and Capacities

	M_f Moment (kN-m)	M_r Resistance (kN-m)
Major Bending	338.2684	1030.365
Minor Bending	44.5768	1030.365

Shear Design

	V_f Force (kN)	V_r Resistance (kN)	Stress Ratio
Major Shear	162.151	2577.96	0.063
Minor Shear	29.4275	2577.96	0.011

Appendix B SMRF and HYBRID Base Shears under 10 Ground Motions

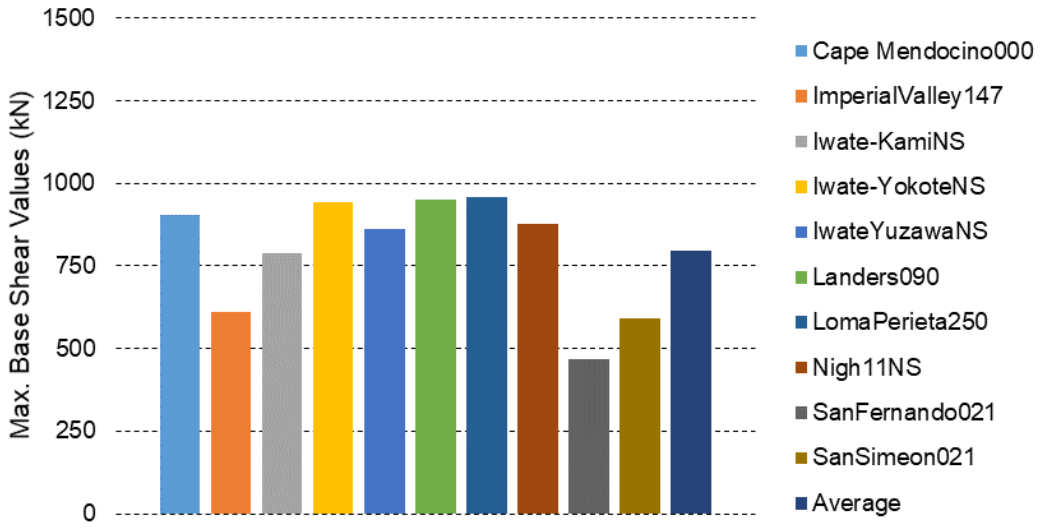

Figure B.1 Maximum base shear during the time history analysis for SMRF 8-Storey model

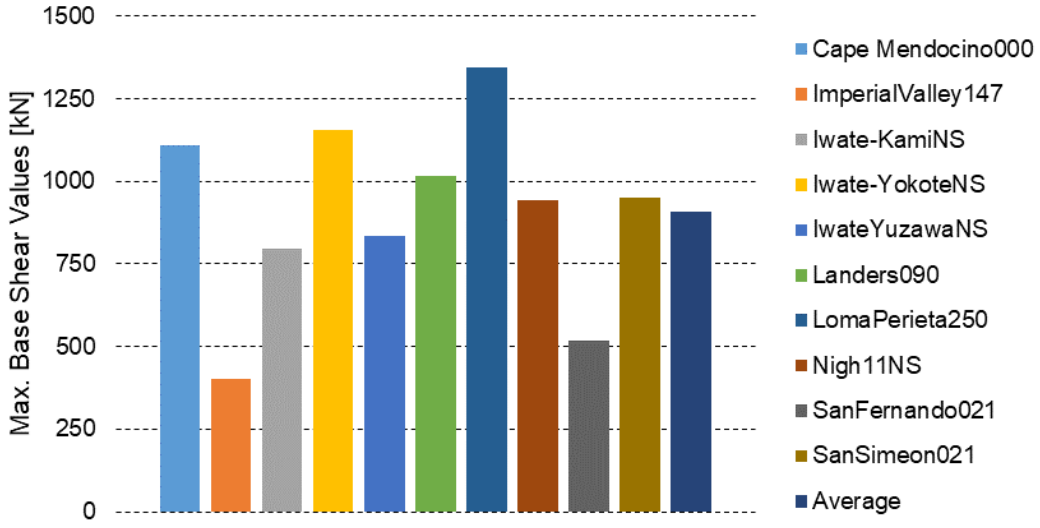

Figure B.2 Maximum base shear during the time history analysis for Hybrid 8-Storey model

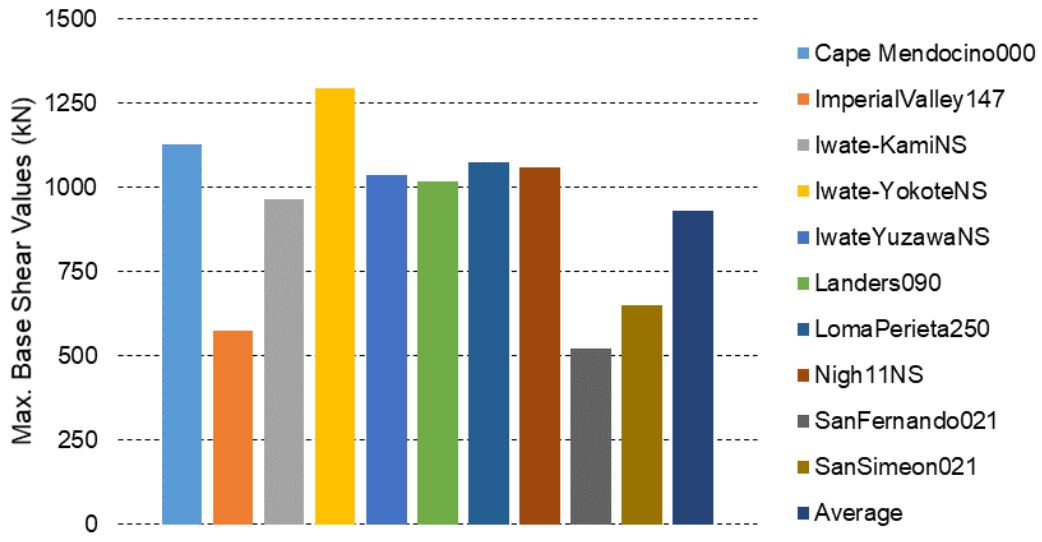

Figure B.3 Maximum base shear during the time history analysis for SMRF 12-Storey model

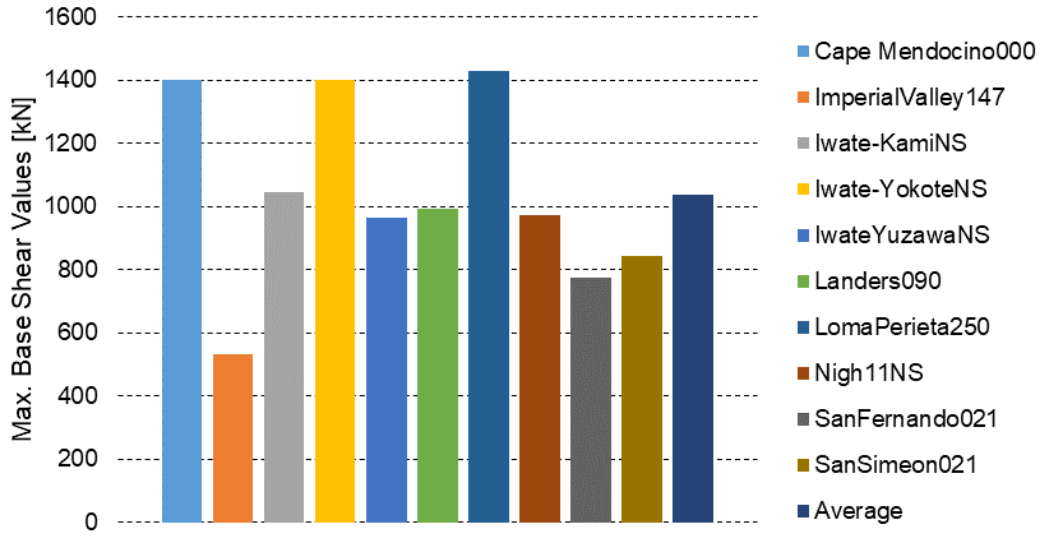

Figure B.4 Maximum base shear during the time history analysis for Hybrid 12 Storey model

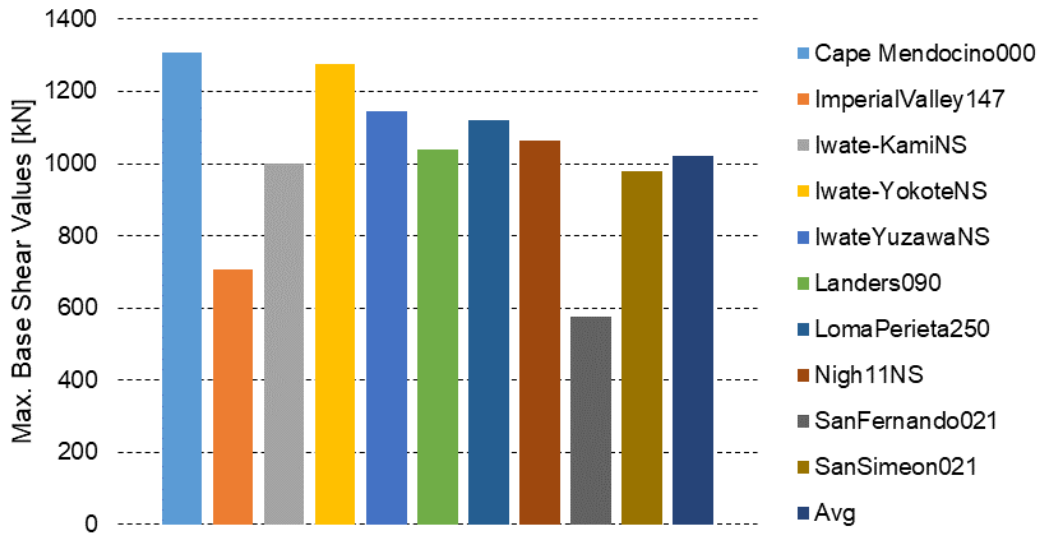

Figure B.5 Maximum base shear during the time history analysis for SMRF 16-Storey model

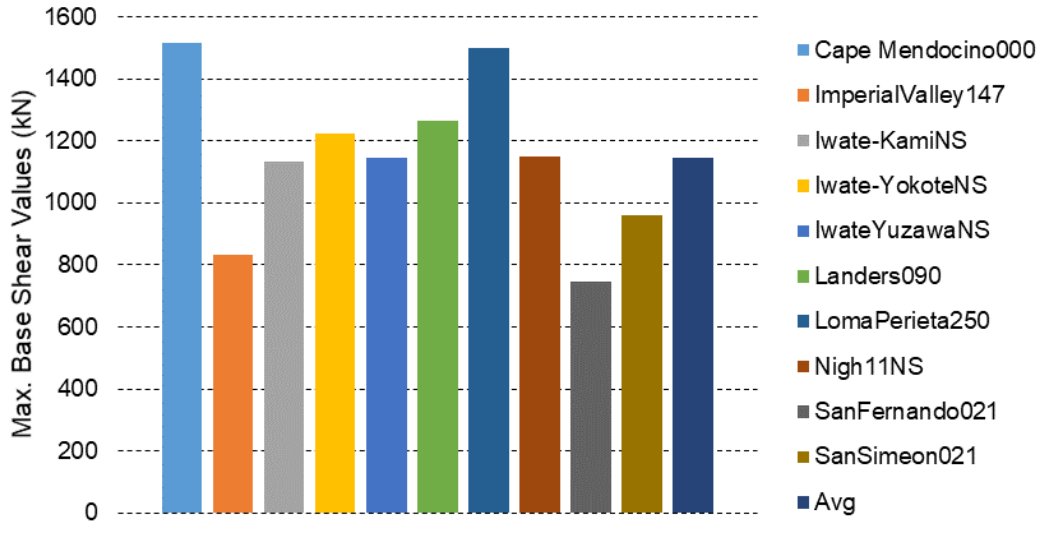

Figure B.6 Maximum base shear during the time history analysis for Hybrid 16-Storey model

Appendix C Distribution of Inter-Storey Drift Over Height of Models

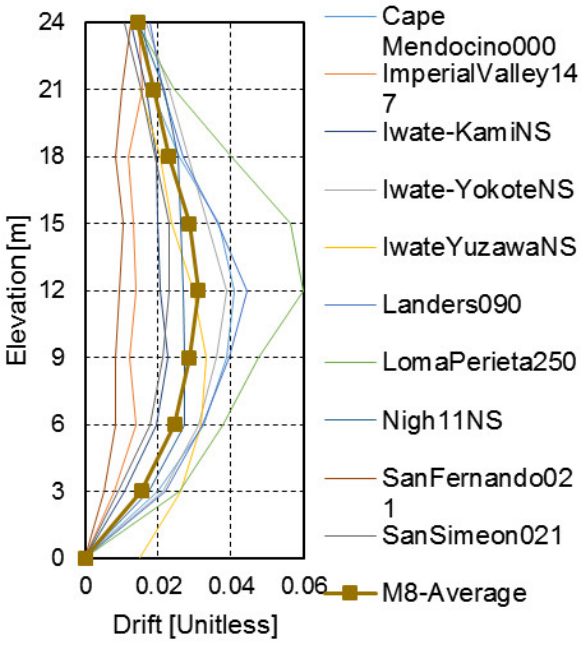

Figure C.1 Inter-Storey drift distribution for ten records for SMRF 8-storey models

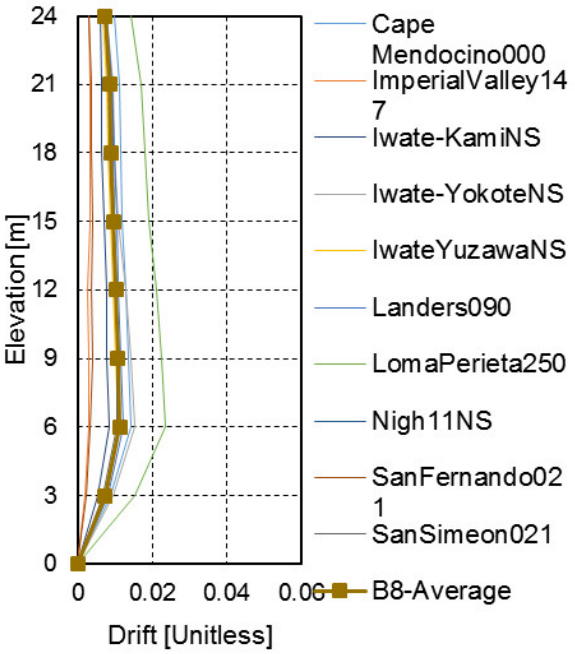

Figure C.2 Inter-Storey drift distribution for ten records for HYBRID 8-storey models

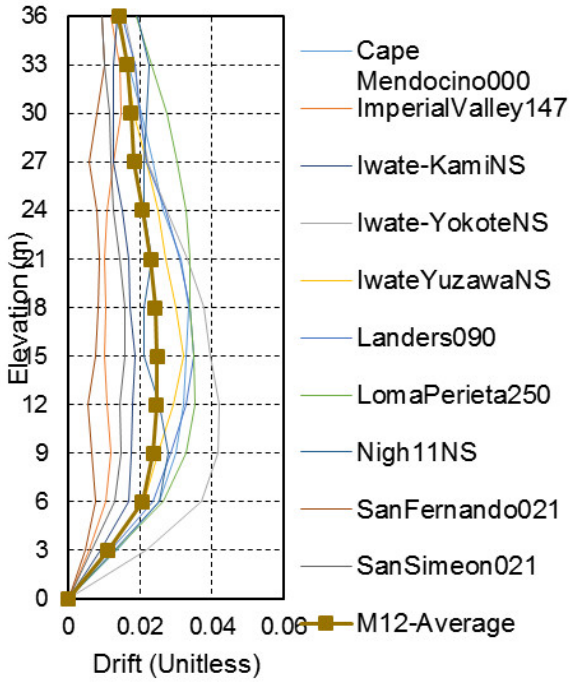

Figure C.3 Inter-Storey drift distribution for ten records for SMRF 12-Storey models

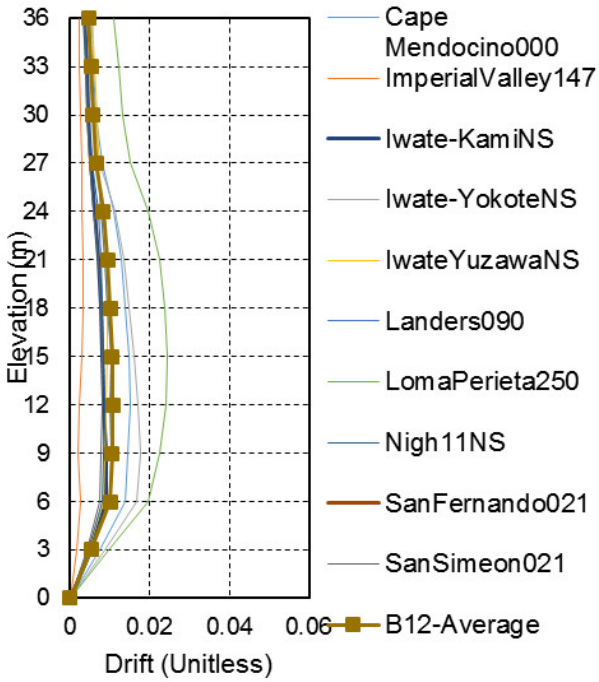

Figure C.4 Inter-Storey drift distribution for ten records for HYBRID 12-Storey models

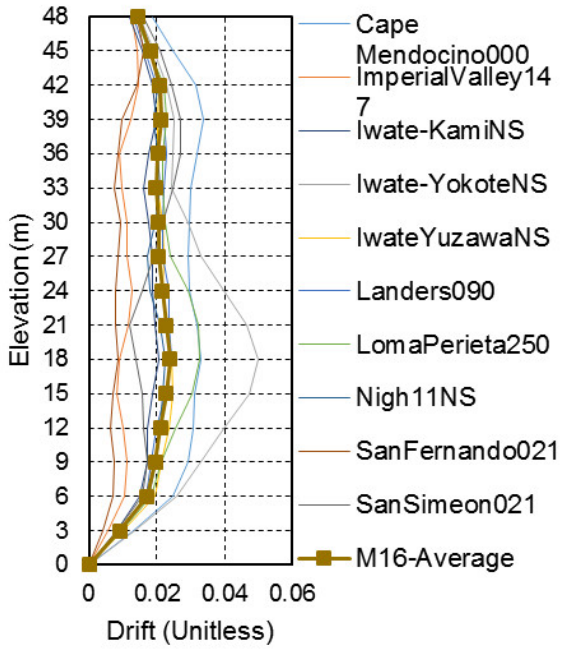

Figure C.5 Inter-Storey drift distribution for ten records for SMRF 16-Storey models

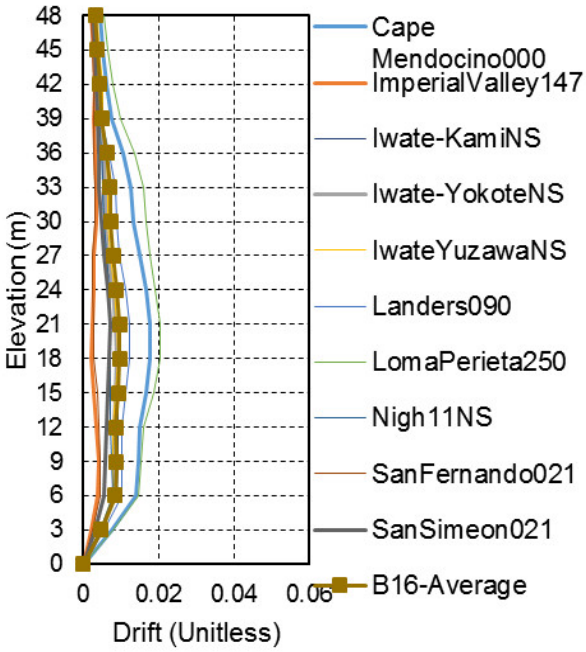

Figure C.6 Inter-Storey drift distribution for ten records for HYBRID 16-Storey models

Appendix D Maximum Forces in HLD1 Hold-down

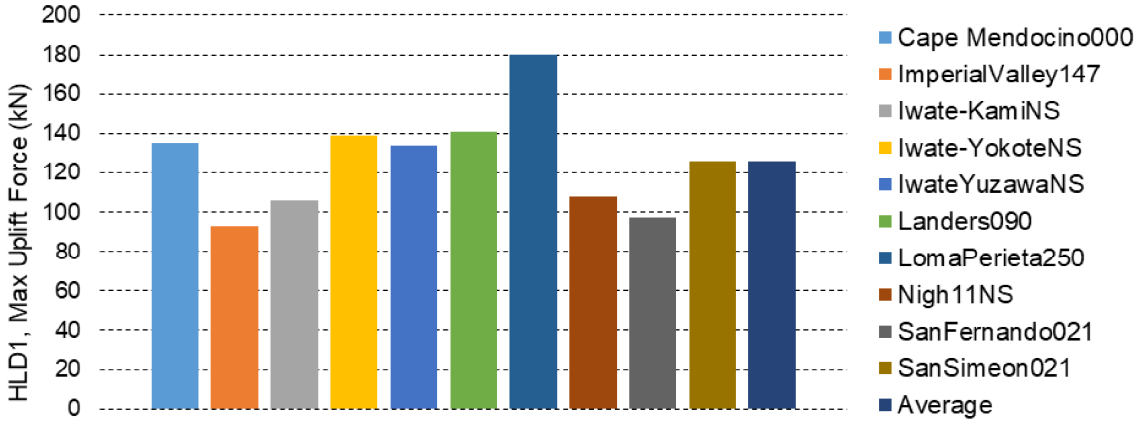

Figure D.1 Max Uplift Force of HLD 1 for 8-storey Hybrid Model

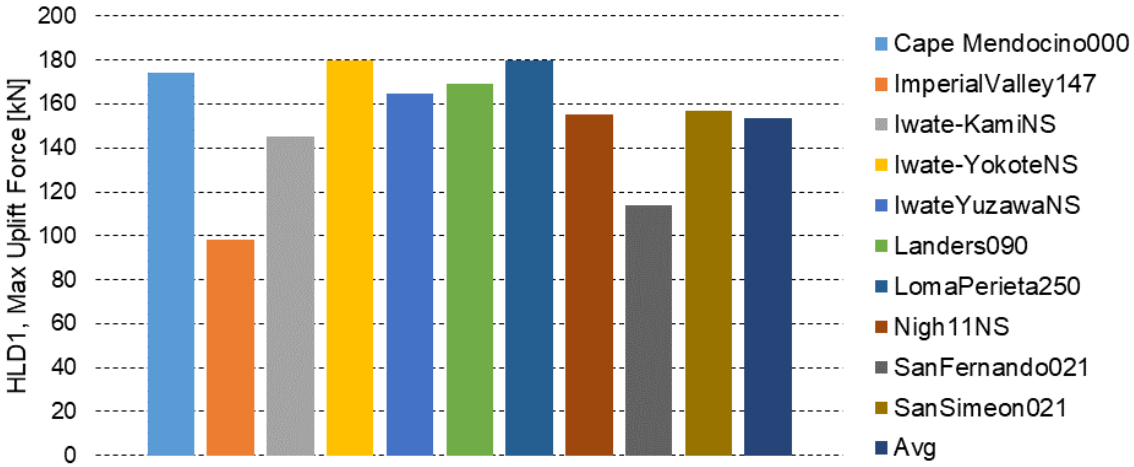

Figure D.2 Max Uplift Force of HLD 1 for 12-Storey Hybrid Model

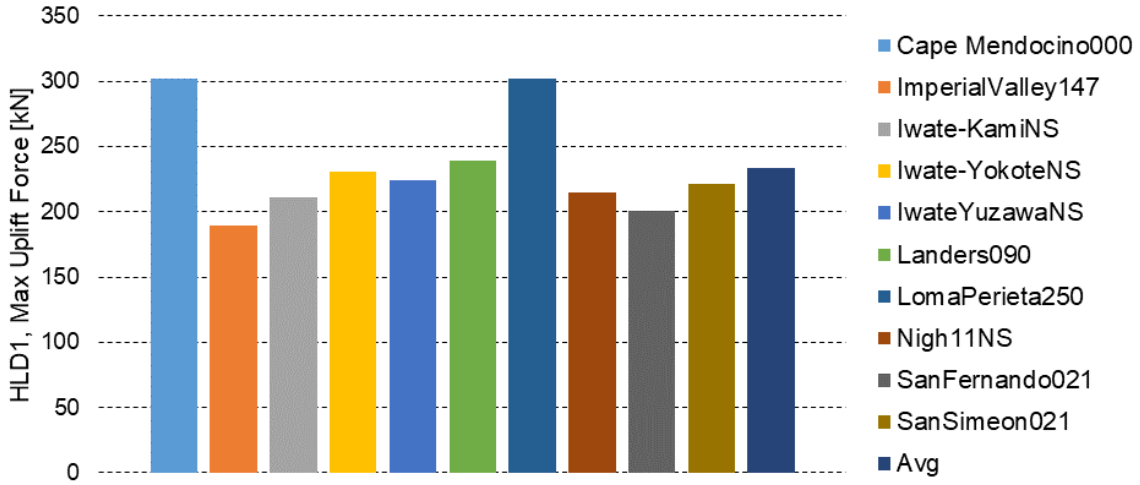

Figure D.3 Max Uplift Force of HLD 1 for 16-Storey Hybrid Model